


## Article

# Concurrent Activation of Both Survival-Promoting and Death-Inducing Signaling by Chloroquine in Glioblastoma Stem Cells: Implications for Potential Risks and Benefits of Using Chloroquine as Radiosensitizer

Andreas Müller<sup>1</sup>, Patrick Weyerhäuser<sup>2</sup>, Nancy Berte<sup>1</sup>, Fitriasari Jonin<sup>1</sup>, Bogdan Lyubarskyy<sup>1</sup>, Bettina Sprang<sup>1</sup>, Sven Rainer Kantelhardt<sup>1</sup>, Gabriela Salinas<sup>3</sup>, Lennart Opitz<sup>4</sup>, Walter Schulz-Schaeffer<sup>5</sup>, Alf Giese<sup>1</sup> and Ella L. Kim<sup>1,\*</sup>

<sup>1</sup> Experimental Neurooncology Group, Clinic for Neurosurgery, Johannes Gutenberg University Medical Centre, 55131 Mainz, Germany; mandre@students.uni-mainz.de (A.M.)

<sup>2</sup> Institute of Toxicology, Johannes Gutenberg University Medical Centre, 55131 Mainz, Germany; patrickwey@web.de

<sup>3</sup> NGS Integrative Genomics Core Unit (NIG), Institute for Human Genetics, University Medical Centre, 37075 Göttingen, Germany; gsalina@gwdg.de

<sup>4</sup> Functional Genomics Center Zurich, ETH Zurich, University of Zurich, 8092 Zurich, Switzerland; lennart.opitz@fgcz.ethz.ch

<sup>5</sup> Department of Neuropathology, Medical Faculty, Saarland University, 66123 Homburg, Germany; walter.schulz-schaeffer@uks.eu

\* Correspondence: ella.kim@unimedizin-mainz.de; Tel.: +49-(0)6131-17-8211



**Citation:** Müller, A.; Weyerhäuser, P.; Berte, N.; Jonin, F.; Lyubarskyy, B.; Sprang, B.; Kantelhardt, S.R.; Salinas, G.; Opitz, L.; Schulz-Schaeffer, W.; et al. Concurrent Activation of Both Survival-Promoting and Death-Inducing Signaling by Chloroquine in Glioblastoma Stem Cells: Implications for Potential Risks and Benefits of Using Chloroquine as Radiosensitizer. *Cells* **2023**, *12*, 1290. <https://doi.org/10.3390/cells12091290>

Academic Editor: Swapan K. Ray

Received: 26 March 2023

Revised: 25 April 2023

Accepted: 27 April 2023

Published: 30 April 2023



**Copyright:** © 2023 by the authors. Licensee MDPI, Basel, Switzerland. This article is an open access article distributed under the terms and conditions of the Creative Commons Attribution (CC BY) license (<https://creativecommons.org/licenses/by/4.0/>).

**Abstract:** Lysosomotropic agent chloroquine was shown to sensitize non-stem glioblastoma cells to radiation in vitro with p53-dependent apoptosis implicated as one of the underlying mechanisms. The in vivo outcomes of chloroquine or its effects on glioblastoma stem cells have not been previously addressed. This study undertakes a combinatorial approach encompassing in vitro, in vivo and in silico investigations to address the relationship between chloroquine-mediated radiosensitization and p53 status in glioblastoma stem cells. Our findings reveal that chloroquine elicits antagonistic impacts on signaling pathways involved in the regulation of cell fate via both transcription-dependent and transcription-independent mechanisms. Evidence is provided that transcriptional impacts of chloroquine are primarily determined by p53 with chloroquine-mediated activation of pro-survival mevalonate and p21-DREAM pathways being the dominant response in the background of wild type p53. Non-transcriptional effects of chloroquine are conserved and converge on key cell fate regulators ATM, HIPK2 and AKT in glioblastoma stem cells irrespective of their p53 status. Our findings indicate that pro-survival responses elicited by chloroquine predominate in the context of wild type p53 and are diminished in cells with transcriptionally impaired p53. We conclude that p53 is an important determinant of the balance between pro-survival and pro-death impacts of chloroquine and propose that p53 functional status should be taken into consideration when evaluating the efficacy of glioblastoma radiosensitization by chloroquine.

**Keywords:** chloroquine; glioblastoma radiosensitization; glioblastoma stem cells; p53; p21-DREAM; ATM; AKT; HIPK2

## 1. Introduction

Glioblastoma (GB) is the most malignant form of brain tumors in adults. With ~15 months survival, GB is associated with one of the poorest clinical outcomes among all human cancers [1–4]. The international standard of care for GB encompasses surgical debulking, followed by hypofractionated radiation (frRT) combined with the alkylating agent temozolomide (TMZ) [5,6]. A high degree of intrinsic and acquired radioresistance is the major

challenge to anti-GB therapy with the need for effective radiosensitizing treatments remaining unmet. GBs are genetically complex tumors characterized by multiple alterations in key pathways that control cellular fate via diverse but functionally overlapping molecular mechanisms [7,8]. The biological paradigm of GB is based on a premise that malignant progression of GB is driven by so-called glioblastoma stem-like cells (GSCs), implicated as the major cellular determinants of GB radioresistance and tumor re-growth after (or under) cytotoxic treatments [9]. Owing to stemness properties and high degree of intrinsic plasticity, manifested in the ability to switch reversibly between distinct cellular states, GSCs are capable of adapting and surviving the impacts of cytotoxic treatments that are otherwise effective against glioma cells lacking stemness properties. Augmented DNA damage response (DDR) and highly efficient DNA repair is of particular importance for the ability of GSCs to withstand clinically relevant exposure to ionizing radiation (IR) [10]. There is a growing consensus that interference with GSC-associated radioresistance is a prerequisite for improving clinical outcomes in patients with GB [9,11]. In this regard, the pleiotropic agent chloroquine (CIQ) has attracted considerable attention for its potential radiosensitizing effects [12,13]. There is some clinical evidence that addition of CIQ to standard therapy can improve clinical outcomes in patients with newly diagnosed and recurrent GB [14–17]. While clinical studies are underway to evaluate the potential merits of CIQ as a radio- or chemosensitizing agent for GB [18–26], there is still a lack of certainty about the molecular and cellular mechanisms underlying anti-tumor actions of CIQ. Although there is considerable experimental evidence indicating that CIQ inhibits glioma cell growth *in vitro*, the molecular factors that determine glioma cell responsiveness to CIQ remain elusive. Up until recently, autophagic inhibition was widely considered to be the major mechanism underlying cancer cell death from CIQ. However, this view has been recently challenged by the results from independent studies addressing the relationship between the tumor-suppressing effects of CIQ and its ability to inhibit autophagy [27–29]. Large-scale investigations conducted by Pfizer, Novartis and AstraZeneca have provided compelling evidence that CIQ-induced cytotoxicity is unrelated to the autophagic inhibition by CIQ [28,29]. These unexpected findings reinforce efforts towards elucidating the mechanisms of CIQ-mediated radiosensitization and its determining molecular factors in particular. Activation of the p53 pathway has been implicated as one of the molecular mechanisms of CIQ-mediated cytotoxicity in different types of cancer cells, including non-stem glioma cells [30–34]. The impacts of CIQ on GSCs and the role of the p53 pathway in CIQ-mediated cytotoxicity are less clear. Considering that p53 is mutationally inactivated in more than 50% of GBs [35] and that some TP53 mutations result in gained activities distinct from those of the wtp53 protein [36–39], an important question is whether the mutational status of p53 has a role in determining cellular outcomes elicited by CIQ. Another source of uncertainty in translating experimental data into clinical practice is the diversity of cellular models and experimental conditions used in different studies. Up till now, CIQ's potential to suppress glioma cells growth has been evaluated exclusively *in vitro* using variable cell culture conditions, mostly those that promote loss of stemness. Furthermore, the radiosensitizing potential of CIQ has been evaluated in the context of a single exposure to relatively high doses of ionizing radiation (IR) using experimental regimens that differ from multifractionated low-dose radiotherapy for GB [40]. Considering that radiation dose is a critical parameter of tumor radioresponsiveness, evaluation of the radiosensitizing potential of CIQ *in vivo* using clinically relevant doses of radiation is a matter of clinical importance.

In this study, *in vitro* and *in vivo* responses mediated by CIQ alone or in combination with clinically relevant doses of IR were evaluated in patient-derived GSCs differing for the status of p53.

## 2. Materials and Methods

### 2.1. Cells and Cell-Based Assays

Human GSC lines used in this study derive from newly diagnosed GB tissues and have been extensively characterized in previous studies [41–45]. The GSC line #993 has an intact TP53 gene whereas #1095 GSCs carry a nonsense mutation, generating a premature stop codon at position 146 (Supplementary Materials Figure S1a,b). G112SP GSCs have been isolated from a glioblastoma cell line G112 and carry a hot-spot mutation R273H [46]. All GSCs used in the study possess the capacity to self-renew in vitro (Figure S1c), capable of initiating and sustaining tumor growth in vivo and recapitulating a highly invasive phenotype of GB (Figure S1d). In vitro cultivation of GSCs was performed using NeuroBasal medium, supplemented with the B27 component (Invitrogen Life technologies, Carlsbad, CA, USA), basic fibroblast growth factor (bFGF) and epidermal growth factor (EGF) (10 and 20 ng/mL, respectively, Biochrom GmbH, Merck KGaA, Darmstadt, Germany). For immunofluorescence staining, GSC spheres were dissociated using Trypsin (Gibco, Thermo Fischer Scientific, Darmstadt, Germany, Cat. #25300-054) diluted at a 1:1 ratio in NeuroBasal medium, plated on ornithin-coated glass coverslips at 30,000 cells/coverslip and allowed to adhere for at least 24 h. Cells were fixed with 4% paraformaldehyde, washed 3 times with PBS and incubated in blocking solution (0.1% Triton X-100, 1% bovine serum albumin) and stained overnight at +4 °C with primary antibodies diluted in blocking solution. Primary antibodies used in the study include  $\alpha$ -Ki67 (Abcam, Cambridge UK, ab16667),  $\alpha$ -nestin (Abcam, Cambridge UK, ab22035), and  $\alpha$ -GFAP (Dako, Hamburg, Germany, Z0334). Secondary antibodies were goat  $\alpha$ -mouse Alexa Fluor 488 (Invitrogen, Carlsbad, CA, USA, A-11001, 1:10,000) or goat  $\alpha$ -rabbit Alexa Fluor 555 (Invitrogen, Carlsbad, CA, USA, A-21429).

### 2.2. Cell Treatments and Cell-Based Assays

Single cell suspensions of GSCs were prepared one day before treatment and treated with freshly prepared CIQ (Sigma-Aldrich, St. Louis, MO, USA, C6628-25G) at 30  $\mu$ M/L for desired time points. For in vitro irradiation, cells were subjected to 2.5 Gy of X-rays using a Gulmay RS225 GS014 X-ray machine (Gulmay Medical Ltd., Camberley, UK) at a dose rate of 1 Gy/min. For flow cytometry,  $2 \times 10^5$  cells either untreated or untreated were harvested at indicated time points after treatment, washed in PBS and pelleted at 1500 rpm and +4 °C for 8 min. Washed cells were re-suspended in PBS, fixed with ice-cold 70% ethanol on the vortex and incubated for 15 min on ice. For staining, cells were rehydrated in PBS, stained using the FxCycle™ PI/RNase Staining Solution Kit (Invitrogen) and processed for flow cytometric analysis of DNA content using the FACSCanto™ Iia (BD, Franklin Lakes, NJ, USA) instrument. Statistical analyses were performed using the GraphPad Prism Version 7 (GraphPad Software Inc., San Diego, CA, USA). Self-renewal was assessed by using the extreme limited dilution assay (ELDA) [47].

### 2.3. Animal Experiments

Animal experiments were conducted in accordance with the guidelines of the European Convention for the Protection of Vertebrates Used for Scientific Purposes under the permission from the State Office of Lower Saxony (permission #33.942502-04/012/07) and State Office of chemical investigations of Rhineland-Palatinate (permission #23 177-07/G12-1-020). The protocol for animal experiments was approved by the Central Animal Research Facility (ZTE) of the University Medical Centre of Göttingen and Translational Animal Research Center (TARC) of the Johannes Gutenberg University Medical Centre of Mainz. Intracranial implantation using immunodeficient mice (NMRI, female, 5–6 weeks old, Charles River Europe) was performed under standardized conditions as described previously [30,42,48]. In brief, single cell suspensions were PBS-washed and re-suspended in PBS at  $3 \times 10^4$  cells/ $\mu$ L. Cell viability was ascertained by using the trypan blue assay. A total of  $10^5$  cells were implanted into the right brain hemisphere using a stereotactic frame (TSE Systems, Bad Homburg, Germany) at 1 mm anteroposterior axis, 3 mm lateromedial

axis, and 2.5 mm vertical axis, relative to bregma. Three weeks after implantation, mice were divided into four groups ( $n = 12/\text{group}$ ) and subjected to single treatments with CIQ or radiation or combined treatment with CIQ and radiation (Figure S2a). CIQ treatment was performed one day before irradiation using an intraperitoneal (i.p.) injection of freshly prepared CIQ in 0.9% NaCl (14 mg/kg). Mice from the control group were injected with 0.9% NaCl without CIQ. Prior to irradiation, mice were anesthetized with an i.p. injection of avertine at 0.4 g/kg body weight, placed in a prone position and covered with 5 mm-thick lead plates containing a rectangular window to allow brain radiation while shielding the rest of body (Figure S2b). Mice were subjected to selective brain radiation with 2.5 Gy using a Varian Clinac 600 C accelerator (dose rate 1 Gy/min). Radiation treatment was performed for 6 consecutive days (2.5 Gy per day). Control (“sham treatment”) or “CIQ only” groups were subjected to the same anesthesia protocol but did not receive irradiation. Mice termination was performed at the onset of tumor-associated neurological symptoms such as seizure, loss of balance, disorientation, and complete or partial paralysis. Mouse brains were isolated, fixed in 4% paraformaldehyde, embedded into paraffin blocks and sectioned for histological analyses. Brain tumors were confirmed by histological examinations of 3  $\mu\text{m}$  sections using hematoxylin-eosin staining and analyzed by immunohistochemical of immunofluorescence staining using antibodies against human nestin (Invitrogen, Thermo Fischer Scientific, Darmstadt, Germany, PA5-82905), glial fibrillary acidic protein (GFAP) (DAKO, Z0334), or KI67 (Abcam; ab16667). For mouse survival studies, statistical analysis was performed using the log-rank (Mantel–Cox) test or Gehan–Breslow–Wilcoxon test. A  $p$  value  $< 0.05$  was considered statistically significant.

#### 2.4. Protein Analyses

Cells were lysed in SDS lysis buffer (1% SDS, 1 mM Tris, 1mM EDTA, and pH 8.0) supplemented with a protease inhibitors cocktail (cComplete™, Sigma-Aldrich) for 10 min at 95 °C and subjected to ultrasound sonification using an Ultrasonicator (Bandelin Sonopuls). After sonification, cell lysates were cleared by centrifugation at 14,000 rpm for 15 min at +4 °C. Protein concentration was determined by using the NanoDrop spectrophotometer (NanoDrop Technologies Inc, Wilmington, DE, USA). Electrophoretic protein separation was achieved by using the precast gels mini-PROTEAN® TGX™ (Bio-Rad, Feldkirchen, Germany) followed by proteins transfer on a PVDF membrane (Thermo Fischer Scientific GmbH, Darmstadt, Germany). Antibodies against p53, p21, p53Ser46P, ATM, ATMSer1981P, AKT, AKTSer473P, HIPK2, LC3B-I, LC3B-II or p62 were from Cell Signaling Technology Inc., Danvers, MA, USA. Other antibodies used were a-p53Ser15P (Proteintech Germany GmbH, Planegg-Martinsried, Germany), a-HIPK2Tyr361P (MyBioSource Inc, San Diego, CA, USA), a-actin (Santa Cruz Biotechnology, Inc., Dallas, TX, USA) or a-HSP70 (Enzo Life Sciences Inc., Farmingdale, NY, USA). On-array protein analyses were performed using the human apoptosis antibody array AAH-APO-G1-8 (RayBiotech Inc., Peachtree Corners, GA, USA) according to the supplier’s recommendations. In brief, cell lysates were prepared from  $2 \times 10^6$  cells and incubated with the array slide overnight at +4 °C on the rotating platform to allow proteins to bind to the array. After the binding step, arrays were washed and subjected to another round of incubation with a cocktail of biotinylated antibodies against apoptosis-related proteins, washed, and incubated with fluorescence dye. Fluorescence signals were detected by using X-ray films (Fujifilm Holdings Corporation, Minato, Japan). Signal intensity was quantified by densitometry using ImageJ (<https://imagej.nih.gov>, accessed on 1 February 2023).

#### 2.5. Gene Expression and Bioinformatics

Gene expression was analyzed in three glioblastoma stem cell lines (#993, #1095 and G112) either untreated or treated with CIQ. In addition to CIQ-associated gene expression, transcriptomic changes associated with exposure to IR were also analyzed in line #993. For each line and each condition (treated or untreated), 3 biological replicates were analyzed. RNA isolation, processing, and array-based profiling using GeneChip® Human Gene



1.0 ST Array (Affymetrix) were performed as described previously [43]. In brief, RNA was isolated using the Trizol (Invitrogen, Waltham, MA, USA) method according to the manufacturer's instructions, treated with DNase I (Sigma-Aldrich, St. Louis, MO, USA) and checked for quality using the Agilent 2100 Bioanalyzer (Agilent Technologies, Santa Clara, CA, USA). cDNA was synthesized using the WT Target Labeling and Control Reagents (Affymetrix, Santa Clara, CA, USA) followed by the cleanup using the GeneChip® Sample Cleanup module (Affymetrix). In vitro transcription was conducted using the WT Target Labeling Kit (Affymetrix). Data analysis was performed by using the affy [49] and Limma package [50] of Bioconductor [51]. The data analysis consisted of between-array normalization, probe summary, global clustering and PCA-analysis, fitting the data to a linear model and detection of differential gene expression. To ensure that the intensities had similar distributions across arrays, quantile-normalization was applied to the log<sub>2</sub>-transformed intensity values. As for the summary of probes, a median polish procedure was chosen. Significant changes in the expression of genes between the groups was analyzed by empirical Bayes statistics by moderating the standard errors of the estimated values [52]. The *p*-values obtained from the moderated *t*-statistic were corrected for multiple testing with the Benjamini–Hochberg method [53]. These *p*-value adjustments guarantee a smaller number of false positive findings by controlling the false discovery rate (fdr). For each gene, the null hypothesis suggesting there is no differential expression between degradation levels was rejected when its fdr was lower than 0.05. Samples were assessed in a blinded manner. Gene expression data and results of bioinformatic analyses are deposited in the Gene Expression Omnibus database with the accession number GSE225191. Textual and graphical outputs of the results of cross-comparison between the genes expressed differentially in different experimental groups were performed by using the Whitehead BaRC (<http://barc.wi.mit.edu/tools/>, accessed on 1 February 2023) and Venn Diagram (<https://bioinformatics.psb.ugent.be/webtools/Venn/>, accessed on 1 February 2023) web tools.

### 2.6. Statistical Analysis

In vitro experiments were performed at least three times. Data were evaluated using Student's *t* test and presented as mean ± SD. *p* values ≤ 0.05, ≤ 0.01, ≤ 0.001 or ≤ 0.0001, respectively, were considered statistically significant, very significant, highly significant or most significant. For mouse survival studies using the Kaplan–Meier method statistical analysis was performed using the log-rank test or Gehan–Breslow–Wilcoxon test. A *p* value < 0.05 was considered statistically significant. All statistical analyses were performed using GraphPad Prism (version 6.01).

## 3. Results

### 3.1. Impact of CIQ Alone or in Combination with IR on GSCs Proliferation and Viability In Vitro

CIQ suppresses in vitro proliferation and viability of non-stem glioma cells in the range of 20–50 μM [30,54–56]. To enable a direct comparison with previously published data, CIQ at 30 μM was used for in vitro treatments of GSCs throughout the study. Similarly with the effects of CIQ reported for non-stem glioma cells, CIQ effectively inhibits in vitro proliferation in all GSCs tested (Figures 1 and S3).

The results showed that the degree of CIQ-mediated proliferative inhibition in vitro is comparable or even greater than that induced by clinically relevant doses of ionizing radiation (2.5 Gy). Cell death assessments, using the sub-G1 assay, revealed that CIQ treatment leads to the increase in fractional DNA content in all GSCs tested, albeit to varying degrees, with wtp53 GSCs being the least susceptible to CIQ-induced cell death compared to R273H-p53 and p53 null GSCs (Figures 2 and S4). Vice versa, wtp53 GSCs showed greater radiosensitivity in vitro than R273H-p53 or p53 null GSCs as evidenced by a moderate but significant increase in sub-G1 cells after IR in wtp53 GSCs but not in R273H-p53 or p53 null GSCs. Notably, the combined treatment with CIQ and radiation in vitro failed to significantly augment cell death rates, which were even reduced in wtp53

and p53 null GSCs compared to CIQ treatment alone (Figure 2). R273H-p53 GSCs did show a trend toward increased cell death after combined treatment with CIQ and IR but the difference between CIQ+IR and CIQ alone treatments was not statistically significant (Figures 1 and S4c). Together, these data demonstrate that CIQ is effective in both inhibiting GSC proliferation and inducing GSC death in vitro and indicate that GSCs differing in the status of p53 vary in their susceptibility to CIQ either in a solo setting or in combination with IR.

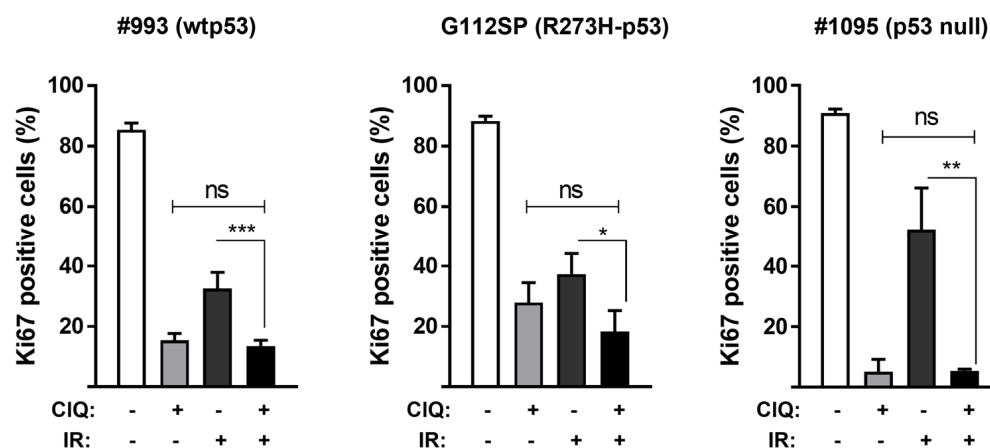


**Figure 1.** Effects of CIQ on GSCs proliferation in vitro. GSCs were treated with CIQ (30  $\mu$ M), irradiation (IR, 2.5 Gy) or combination of CIQ+IR for 72 h and analyzed by immunofluorescence staining for Ki-67. Summary of the data from three independent experiments. Statistical significance was determined using Student’s *t*-test. (\*),  $p \leq 0.05$ ; (\*\*),  $p \leq 0.01$ ; (\*\*\*),  $p \leq 0.001$ . “ns”, not significant.

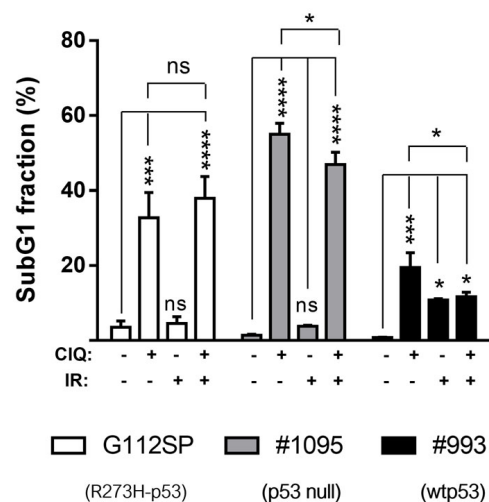


**Figure 2.** Effects of CIQ on GSCs viability in vitro. GSCs were treated with CIQ (30  $\mu$ M), irradiation (IR, 2.5 Gy) or combination of CIQ+IR for 72 h and assessed for the sub-G1 content by flow cytometry. Summary of the data obtained from three independent experiments. Statistical significance was determined by an unpaired *t*-test with Welch’s correction. (\*),  $p \leq 0.05$ ; (\*\*\*),  $p \leq 0.001$ ; (\*\*\*\*),  $p \leq 0.0001$ , “ns”, not significant.

### 3.2. In Vivo Effects of CIQ Alone or in Combination with IR on the Tumor-Propagating Capacity of GSCs

We next sought to determine if the proliferation-inhibiting and death-promoting impacts of CIQ, effective against in vitro propagating GSCs, can be realized in vivo and suppress GSC-driven tumor growth. To that end, CIQ impacts, alone or in combination with clinically relevant doses of hypofractionated IR (frIR, six daily fractions of 2.5 Gy),

were evaluated in GSC xenografts as depicted in Figure S2. In vivo outcomes of frIR treatment showed good concordance with the patterns of GSC radiosensitivity in vitro. Consistent with in vitro radioresistance of p53-R273H and p53 null GSCs (Figure 1), their derived tumors also manifest a radioresistant phenotype (Figure 3a), whereas wtp53 GSCs, showing a greater higher degree of radiation-induced death in vitro (Figure 2), recapitulate a radiosensitive phenotype in vivo (Figure 3a). Unlike frIR, CIQ treatment in vivo poorly reproduces CIQ's efficacy in inhibiting GSC proliferation and viability in vitro as evident from the lack of significant effect of CIQ treatment on xenografted GSCs irrespective of their p53 status (Figure 3b). Moreover, tumors grown from p53-R273H GSCs showed a tendency to grow even faster after the treatment with CIQ (Figure 3b). However, the combined treatment with CIQ and frIR proved effective in retarding p53-R273H tumors as evidenced by a significant ( $p = 0.001$ ) prolongation of survival compared to the sham-treated control group (Figure 3c) or mice treated singly with CIQ or frIR (Figure 3a,b).

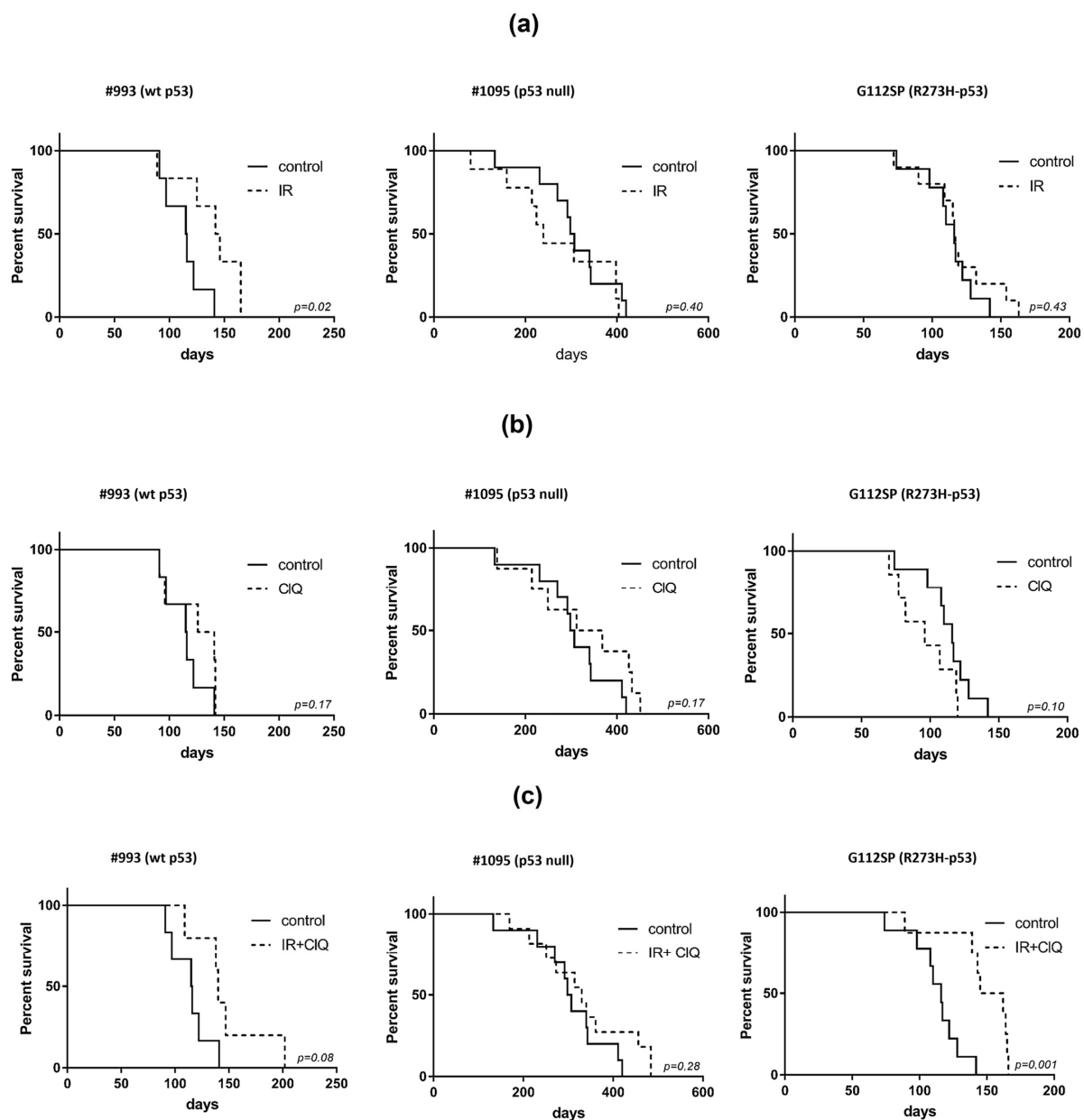


**Figure 3.** Effects of CIQ in vivo. Survival analyses of GSC xenografted mice treated with CIQ (a), radiation (b) or combination of CIQ and IR (c). Solid lines correspond to sham-treated control groups. Kaplan–Meier curves of mice survival were determined using the log-rank test.

In contrast to p53-R273H xenografts, wtp53 or p53 null xenografts showed no significant prolongation of survival after combination treatment with CIQ and frIR compared to single treatments with CIQ or frIR. Together, our *in vivo* data indicate that (i) CIQ is poorly effective in inhibiting the tumor-propagating capacity of GSCs in a single treatment setting; (ii) combination treatment with CIQ and frIR is effective in sensitizing GSC tumors to radiation, but in a differential manner; and (iii) wtp53 does not render GSC tumors more susceptible to CIQ-mediated radiosensitization.

### 3.3. CIQ Elicits Distinct Molecular Outcomes in GSCs Differing for the Status of p53

The p53-dependent and p53-independent mechanisms have been implicated in CIQ-induced death of cancer cells including non-stem glioma cells [30,57–59]. To address the relationship between CIQ and p53 activity in GSCs, we assessed the effects of CIQ on the p53 protein and p53 modulating factors in GSCs expressing wtp53 or R273H-p53 mutant. The results showed that CIQ treatment leads to the accumulation of p53 protein and its transcriptional target p21 in wtp53 GSCs but not in GSCs with transcriptionally impaired mutant R273H-p53 (Figure 4).

Surprisingly, p53 accumulation induced by CIQ is unaccompanied by p53 phosphorylation on key regulatory serines, including Ser46 (Figure 4) or phosphorylation of a p53-specific E3-ligase MDM2 on Ser395, a modification that is required for p53 stabilization after DNA damage (Figure 5).

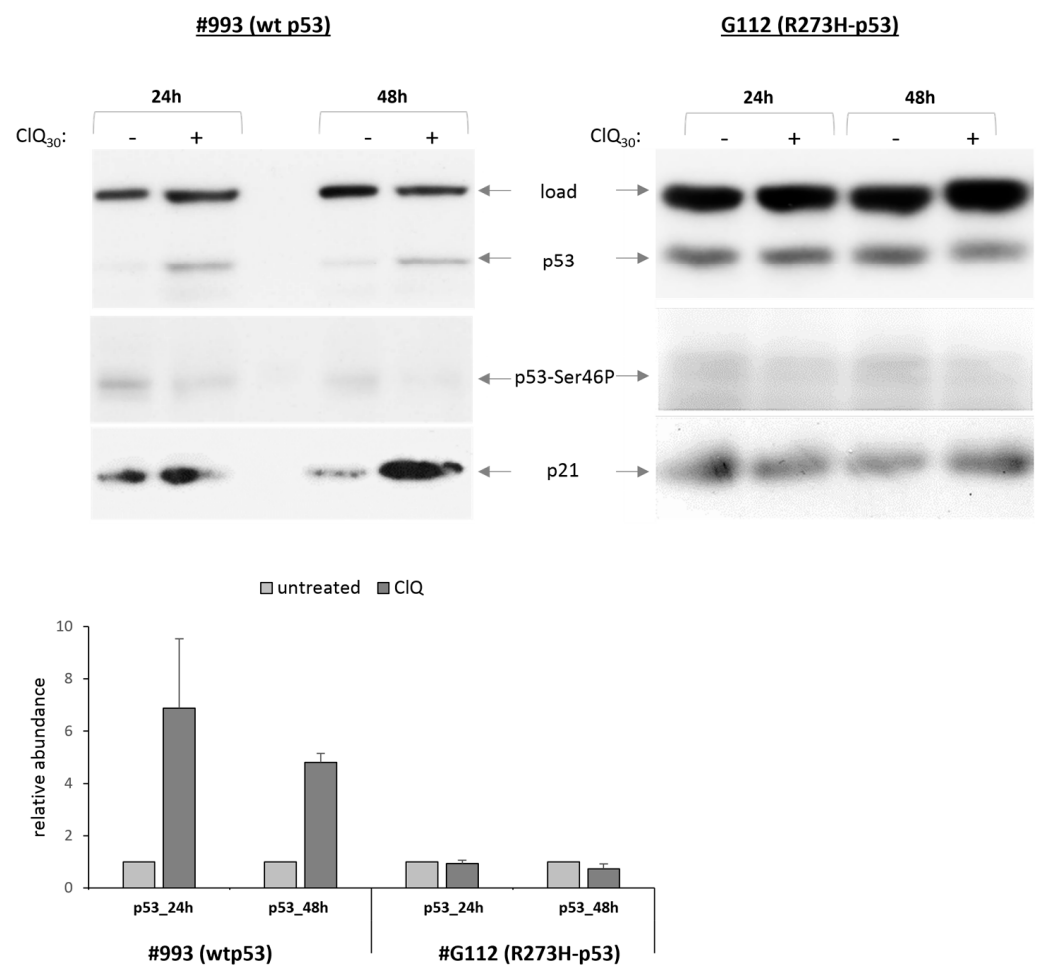
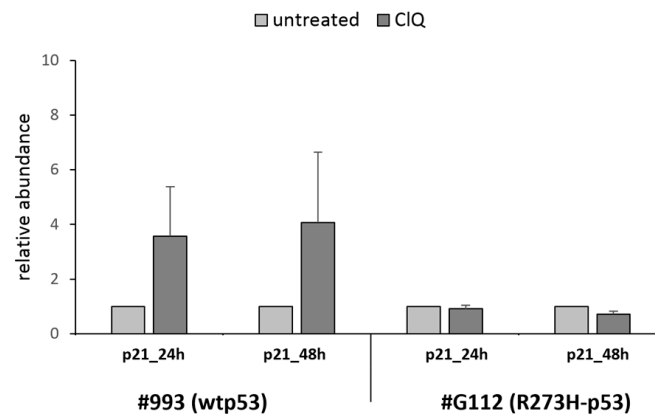
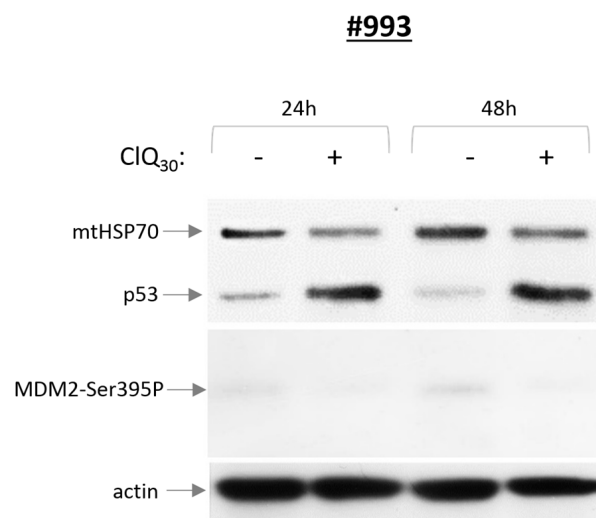


Figure 4. Cont.





**Figure 4.** Effects of CIQ on p53, p53-Ser46P and p21 proteins. Top, representative blots for wtp53 or R273H-p53 expressing GSCs treated with CIQ for 24 h and 48 h. Protein loading was ascertained by probing for the mitochondrial resident mtHSP70. Graph shows quantitative evaluations of p53 and p21 levels by densitometry, in untreated or CIQ-treated GSCs. For total protein normalization, mitochondrial HSP70 or b-actin were used as internal loading controls. Data from three independent experiments were analyzed for each line.



**Figure 5.** Assessment of p53 and MDM2-Ser395P proteins in wtp53 expressing GSCs. Representative blot for wtp53 GSCs treated with CIQ for 24 h and 48 h. Experiments were performed at least three times.

Lack of p53 and MDM2 phosphorylation on serines 46 and 395, respectively, in spite of p53 accumulation induced by CIQ is intriguing considering that these modifications are mediated by the ataxia-telangiectasia mutated (ATM) protein kinase, which is sensitive to CIQ [60] and phosphorylates both p53-Ser46 of p53 and MDM2-Ser395 in response to DNA damage [61–63]. We next sought to clarify if the canonical signaling involved in p53 accumulation induced by DNA damage also operates in CIQ-treated GSCs. While keeping in mind that CIQ treatment induces an activating ATM autophosphorylation on Ser1981 [60] the levels of ATM-Ser1981P were assessed in untreated and CIQ-treated GSCs. Consistent with previous findings that constitutive activation of ATM is a hallmark of GSCs [10], untreated GSCs show considerably higher steady-state levels of ATM-Ser1981P than non-stem glioblastoma cells U87 in which ATM-Ser1981P is barely detectable in the absence of DNA damage but increases upon exposure to radiation (Figure S5).

Strikingly, GSCs treated with CIQ showed a dramatic change in the ATM-Ser1981P pattern characterized by the appearance of smaller ATM-Ser1981P (termed hereafter as  $\Delta$ ATM-Ser1981P) with the apparent molecular weight of ~250 and 100 kDa (Figure 6).

Confirming their ATM origin,  $\Delta$ ATM-Ser1981P forms are recognized by both pan-ATM and ATM-Ser1981P-specific antibodies (Figure S6a). Notably, the truncated ATM forms make a major contribution to the overall increase in Ser1981 phosphorylation levels (Figure 6) indicating that CIQ-induced fragmentation affects preferentially the active, ATM-Ser1981P form. These data thus reveal a duality of CIQ impacts on ATM: on the one hand, CIQ induces an autoactivating phosphorylation of Ser1981 confirming the previous findings of Bakkenist and Kastan [60] but on the other hand, it also promotes ATM-Ser1981P fragmentation, a previously unknown action of CIQ that occurs in all GSCs tested albeit with varying degrees and temporal dynamics (Figures 6 and S6a). CIQ-induced fragmentation of ATM-Ser1981P is a phenomenon specifically associated with CIQ because it does not occur in radiation-treated GSCs (Figure S6b).

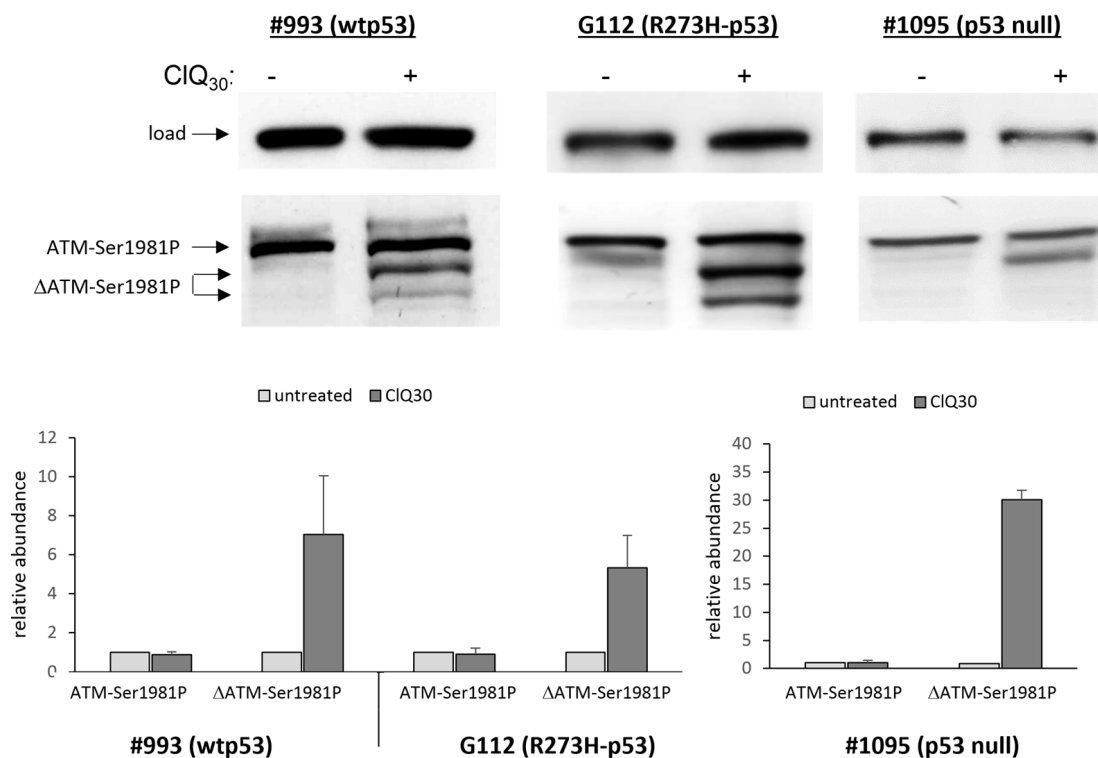


**Figure 6.** Dual effect of CIQ on ATM phosphorylation at Ser1981 and structural integrity of the ATM-Ser1981P protein. Top panel shows representative blots for ATM-Ser1981P in wtp53 (#993), R273H-p53 (G112) or p53-null GSCs after 72 h of treatment with CIQ. Graph shows the results of quantitative evaluations of the full-length and truncated ATM-Ser1981P levels by densitometry ( $n = 3$  for each line). For total protein normalization, mitochondrial HSP70 or b-actin were used as internal loading controls.

It has been shown that ATM fragmentation by proteolytic cleavage is one of the mechanisms inactivating its kinase activity towards Ser46 of the p53 protein in particular [64]. In the light of this knowledge, CIQ-induced fragmentation of ATM might provide a plausible explanation for why wtp53 accumulation induced by CIQ in GSCs is unaccompanied with p53 phosphorylation on Ser46 (Figure 4). However, ATM is not the only kinase that phosphorylates p53 on Ser46, which is also targeted by the homeodomain-interacting protein kinase 2 (HIPK2). HIPK2-mediated phosphorylation of p53-Ser46 is of special interest because it plays a crucial role in transcription of p53-regulated apoptotic genes. Therefore, we have also examined the effect of CIQ on HIPK2. Western blot assessments showed that CIQ treatment leads to a marked decline in the levels of both total HIPK2 and its activated form HIPK2-Tyr361P, which occurred in all tested GSCs irrespective of their p53 status (Figure 7).

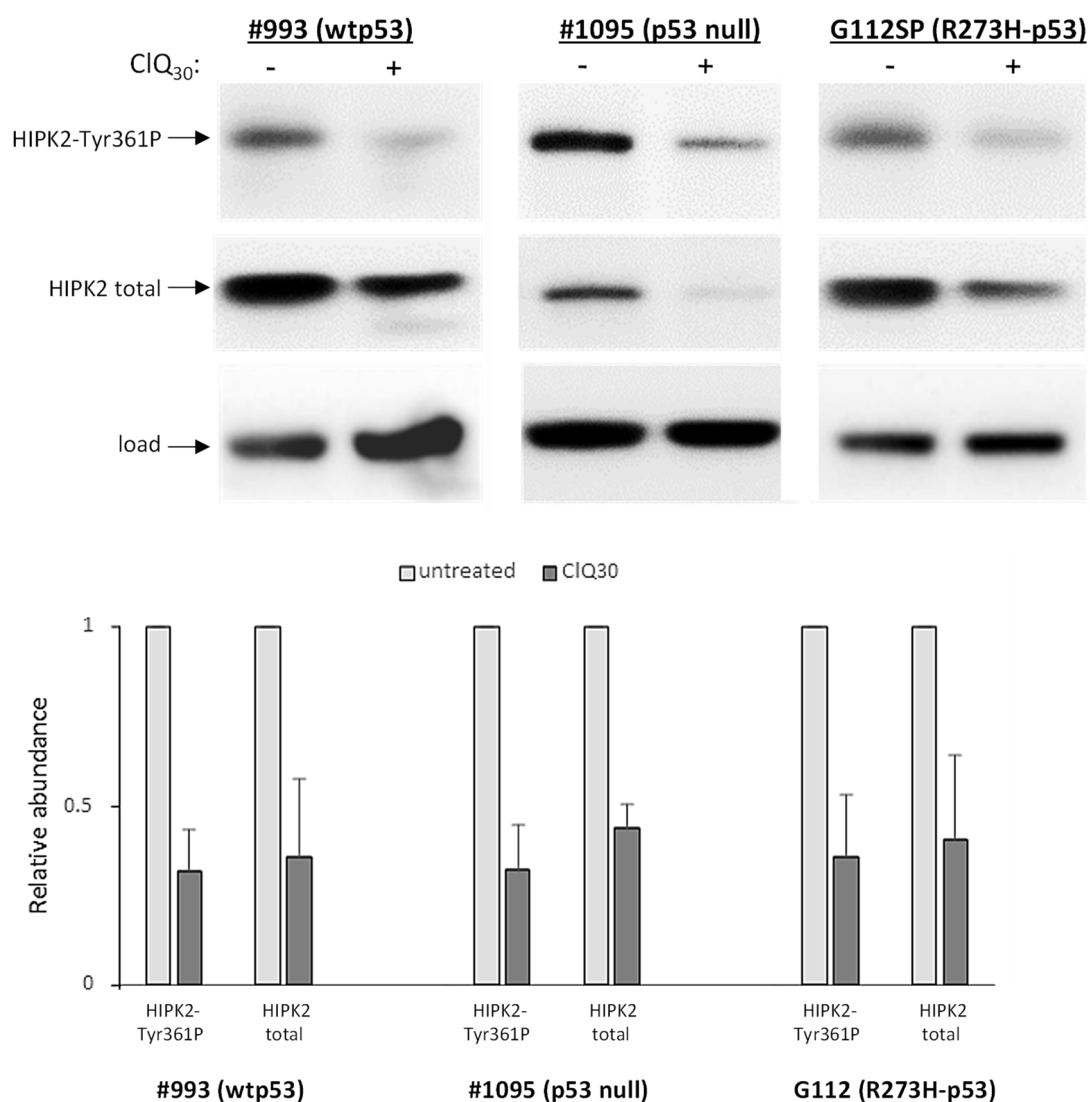


**Figure 7.** Assessments of HIPK2 proteins in GSCs differing for the p53 status. Western blot data for total and Tyr361P phosphorylated HIPK2 in GSCs expressing wtp53 (#993), R273H-p53 (G112) or p53-null GSCs after 72 h of treatment with CIQ. Top panel shows representative blots for total HIPK2 and HIPK2-Tyr361P isoform in wtp53 (#993), R273H-p53 (G112) or p53-null GSCs after 72 h of treatment with CIQ. Graph shows the results of quantitative evaluations by densitometry ( $n = 3$  for each line). For total protein normalization, mitochondrial HSP70 or b-actin were used as internal loading controls.

Altogether these results reveal that in addition to its potential to induce p53 accumulation CIQ also reduces the abundance of p53-regulating kinases ATM and HIPK2 that occurs in GSCs either proficient or deficient for the wtp53 function.

#### 3.4. CIQ Induces Transcriptional Repression via the p53-p21-DREAM Pathway Concurrently with Transcriptional Activation of the Mevalonate Pathway

ATM and HIPK2 kinases are important modulators of p53-mediated transcription, encompassing hundreds of genes [65]. Our finding that CIQ affects the abundance of active ATM and HIPK2 (Figures 6 and 7) prompted us to test the effects of CIQ on p53-dependent transcription. To that end, a microarray-based approach was employed to identify differentially expressed genes influenced by CIQ (termed as “CIQ\_DEGs”). Gene expression analyses revealed that CIQ treatment elicits considerable transcriptional changes in all tested GSCs albeit in varying degrees (Figure 8).

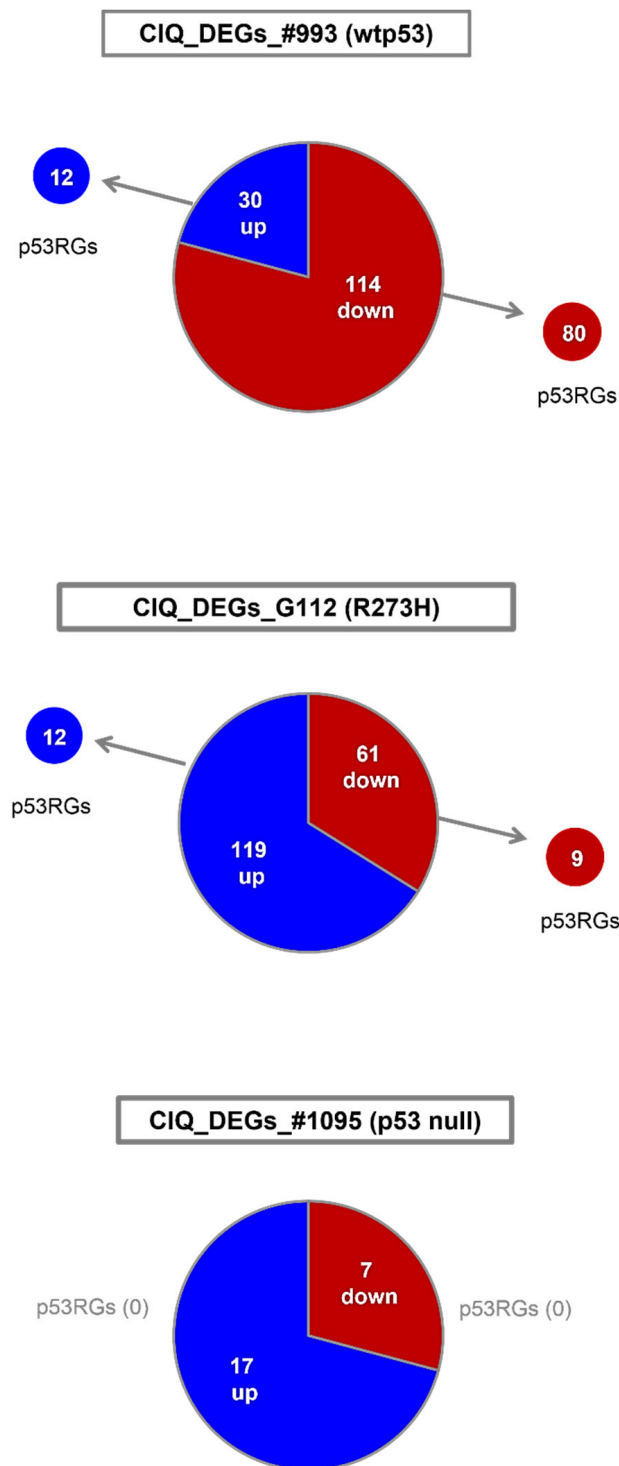


**Figure 8.** Schematic presentation of CIQ\_DEGs identified in GSCs differing for the p53 status. “p53RGs”, p53-regulated genes. “up”, upregulated CIQ\_DEGs. “down”, down-regulated CIQ\_DEGs. Encircled numbers correspond to known p53RGs.

Transcriptional changes induced by CIQ are considerably more profound in wtp53 GSCs and p53-R273H GSCs (144 and 180 differentially expressed genes, respectively, Figures S7 and S8) than in p53 null GSCs (24 genes, Figure S9). The functional spectrum of CIQ\_DEGs also differs markedly between GSCs. In wtp53 GSCs, the majority of CIQ\_DEGs (up-regulated and down-regulated) is constituted by p53 regulated genes (p53RGs), indicating a robust induction of p53-dependent transcriptional response (Figure 8 and Table 1).

The predominance of p53RGs is especially pronounced among down-regulated CIQ\_DEGs, comprised nearly completely by genes from the p21-DREAM pathway, the major mechanism for cell cycle control via p53-dependent transcriptional repression [66–68]. Also, among up-regulated genes, almost half of CIQ\_DEGs are p53RGs from the mevalonate (MVA) pathway associated with cancer cells survival (Table 1), whereas apoptosis-inducing p53RGs are not activated by CIQ.

**Table 1.** Contribution of p53-regulated genes to the transcriptomic response induced by CIQ in GSCs expressing wild type p53. p53RGs, p53-regulated genes; CIQ\_DEGs, chloroquine-induced differentially expressed genes; MVA, mevalonate pathway; GO, Gene Ontology. (\*), p53RGs belonging to the p21-DREAM pathway. (\*\*), p53RGs belonging to the MVA pathway.

CIQ_DEGs_#993 (wtp53)		
p53RGs (80) * p21-DREAM	<b>down-regulated</b>	<b>GO Terms:</b> cell cycle mitosis cytokinesis DDR
	<i>anln</i> *; <i>arhgap11a</i> *; <i>arhgap11b</i> *; <i>aspm</i> *; <i>aurka</i> *; <i>bub1</i> *; <i>bub1b</i> *; <i>casc5</i> *; <i>c11orf82</i> *; <i>c12orf48</i> *; <i>ccdc18</i> *; <i>ccna2</i> *; <i>ccnb1</i> *; <i>ccnb2</i> *; <i>ccne2</i> ; <i>cdc2</i> ; <i>cdca2</i> *; <i>cdca3</i> *; <i>cdca8</i> *; <i>cdc25c</i> *; <i>cdkn3</i> *; <i>cenpe</i> *; <i>cit</i> *; <i>ckap2l</i> *; <i>dc</i> ; <i>depdc1</i> *; <i>depdc1b</i> *; <i>dlgap5</i> *; <i>esco2</i> *; <i>exo1</i> *; <i>fam64a</i> *; <i>fanca</i> *; <i>fancc</i> *; <i>fancl</i> *; <i>gas2l3</i> *; <i>gtse1</i> *; <i>hist1h2bm</i> *; <i>hjurp</i> *; <i>hmmr</i> *; <i>kif2c</i> *; <i>kif4a</i> *; <i>kif11</i> *; <i>kif14</i> *; <i>kif15</i> *; <i>kif18a</i> *; <i>kif20a</i> *; <i>kif20b</i> *; <i>kif23</i> *; <i>kif24</i> *; <i>mad2l1</i> *; <i>melk</i> *; <i>mki67</i> *; <i>ncapg</i> *; <i>ncapg2</i> *; <i>ncaph</i> *; <i>ndc80</i> *; <i>neil3</i> *; <i>nuf2</i> *; <i>nusap1</i> *; <i>plk1</i> *; <i>plk4</i> *; <i>polq</i> *; <i>prc1</i> *; <i>prr11</i> *; <i>pttg1</i> *; <i>racgap1</i> *; <i>rrm2</i> ; <i>rtnk2</i> *; <i>sema3a</i> ; <i>sgol1</i> *; <i>sgol2</i> *; <i>shcbp1</i> *; <i>spag5</i> *; <i>spc25</i> *; <i>stil</i> *; <i>top2a</i> *; <i>tpx2</i> *; <i>troap</i> *; <i>ttk</i> *; <i>ube2c</i> *; <i>xrcc2</i> *	
p53RGs (12) ** MVA	<b>up-regulated</b>	<b>GO Terms:</b> lipid metabolism cholesterol- biosynthesis
	<i>acat2</i> **; <i>dhcr7</i> **; <i>dhcr24</i> **; <i>fasn</i> **; <i>fdft1</i> **; <i>fdps</i> **; <i>lpin1</i> **; <i>lss</i> **; <i>mvd</i> **; <i>nsdhl</i> **; <i>sc4mol</i> **; <i>tm7sf2</i> **	

Consistently with impairment of transcriptional activity in mutant p53 proteins, p53RGs constitute only a minor fraction of all CIQ\_DEGs identified in GSCs that express R273H-p53 (Table 2).

**Table 2.** Contribution of p53-regulated genes to the transcriptomic response induced by CIQ in GSCs expressing R273H-p53 mutant. Abbreviations as in Table 1. (\*), p53RGs belonging to the p21-DREAM pathway. (\*\*), p53RGs belonging to the MVA pathway.

CIQ_DEGs_G112 (R273H-p53)		
p53RGs (9) * p21-DREAM	<b>down-regulated:</b>	<b>GO Terms:</b> cell cycle mitosis cytokinesis DDR
	<i>ccnb1</i> *; <i>dlgap5</i> *; <i>exo1</i> *; <i>kif4a</i> *; <i>kif20a</i> *; <i>kif23</i> *; <i>neil3</i> *; <i>sema3a</i> ; <i>top2a</i> *	
p53RGs (7) ** MVA	<b>up-regulated:</b>	<b>GO Terms:</b> lipid metabolism cholesterol- biosynthesis
	<i>dhcr7</i> **; <i>fasn</i> **; <i>fdps</i> **; <i>hmgcr</i> **; <i>hmgcs1</i> **; <i>lss</i> **; <i>sc4mol</i> **	

In p53 null GSCs, the impact of CIQ on transcription is the weakest in terms of both the overall number of CIQ\_DEGs and their dependence on p53 activity, with none of the CIQ\_DEGs identified in p53-null GSCs being a known p53RG (Table 3).

Notably, more than half of up-regulated and nearly all down-regulated CIQ\_DEGs identified in p53-null GSCs are known to be associated with GB progression, resistance to therapy, or GB stemness (Table S1). Collectively, gene expression analyses reveal that (i) CIQ has an influence on both p53-dependent and p53-independent transcription; (ii) p53 status has a decisive impact on the functional spectrum of CIQ-modulated genes; and (iii) p53-regulated genes with pro-survival functions are preferentially impacted by CIQ in wtp53 GSCs.



**Table 3.** Contribution of p53-regulated genes to the transcriptomic response induced by CIQ in GSCs expressing R273H-p53 mutant. Abbreviations as in Table 1. (\*), genes associated with GB promotion.

CIQ_DEGs #1095 (p53 null)		
p53RGs (0) * GB promotion	<b>down-regulated:</b> <i>arhgap29</i> *; <i>id1</i> *; <i>id3</i> *; <i>igfbp5</i> *; <i>itga3</i> * <i>tnfaip3</i> *; <i>trdc</i>	<b>GO Terms:</b> receptor activity migration
p53RGs (0) * GB promotion	<b>up-regulated:</b> <i>acs16</i> *; <i>bhlhe41</i> ; <i>cryab</i> *; <i>ddit4l</i> *; <i>fabp3</i> *; <i>fn3k</i> ; <i>gdf15</i> *; <i>gpnmb</i> *; <i>lipg</i> ; <i>lrrc39</i> ; <i>nckap5</i> *; <i>pcsk6</i> *; <i>pfkfb2</i> *; <i>pi15</i> ; <i>pnliprp3</i> ; <i>serinc5</i> ; <i>st3gal5</i> *	<b>GO Terms:</b> proliferation metabolism

### 3.5. Impacts of CIQ on the Apoptotic Signaling

Our gene expression analysis indicates that apoptosis mediated via p53-dependent transcription is unlikely to be the mechanism of CIQ-induced cell death. To gather further insights into the impacts of CIQ on apoptotic signaling, we made use of the Apoptosis Signaling Array (AAH-APOSIG1, Figure S10). The results showed that CIQ treatment elicits changes in the apoptotic signaling in both wtp53 and R273H-p53 GSCs, albeit to varying degrees. For example, caspase-3 cleavage is quite profound in wtp53 GSCs (Figure 9a) but considerably less effective in R273H-p53 GSCs (Figure 9b). One common change induced by CIQ comparably strongly in wtp53 GSCs and R273H-p53 GSCs is a marked reduction in AKT-Ser473P, an activated form of survival-promoting kinase AKT and its downstream target BAD-Ser112P.

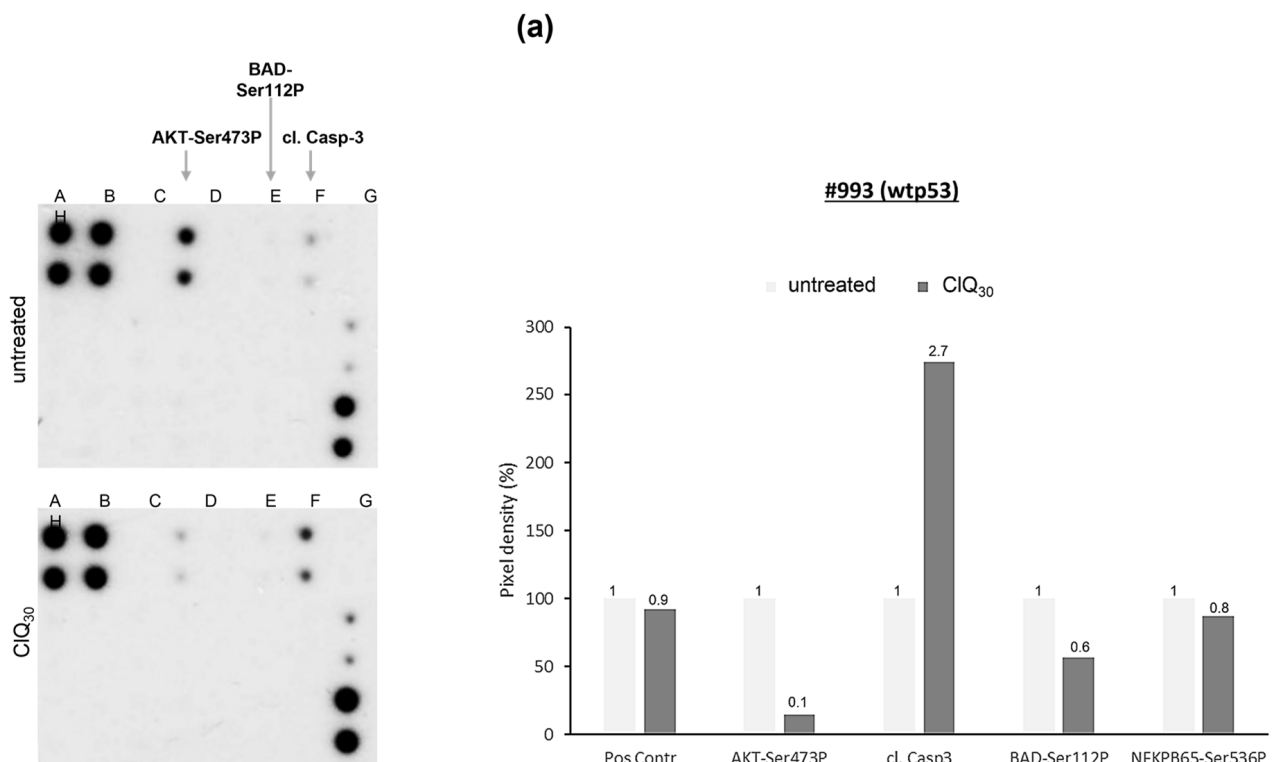


**Figure 9.** Cont.

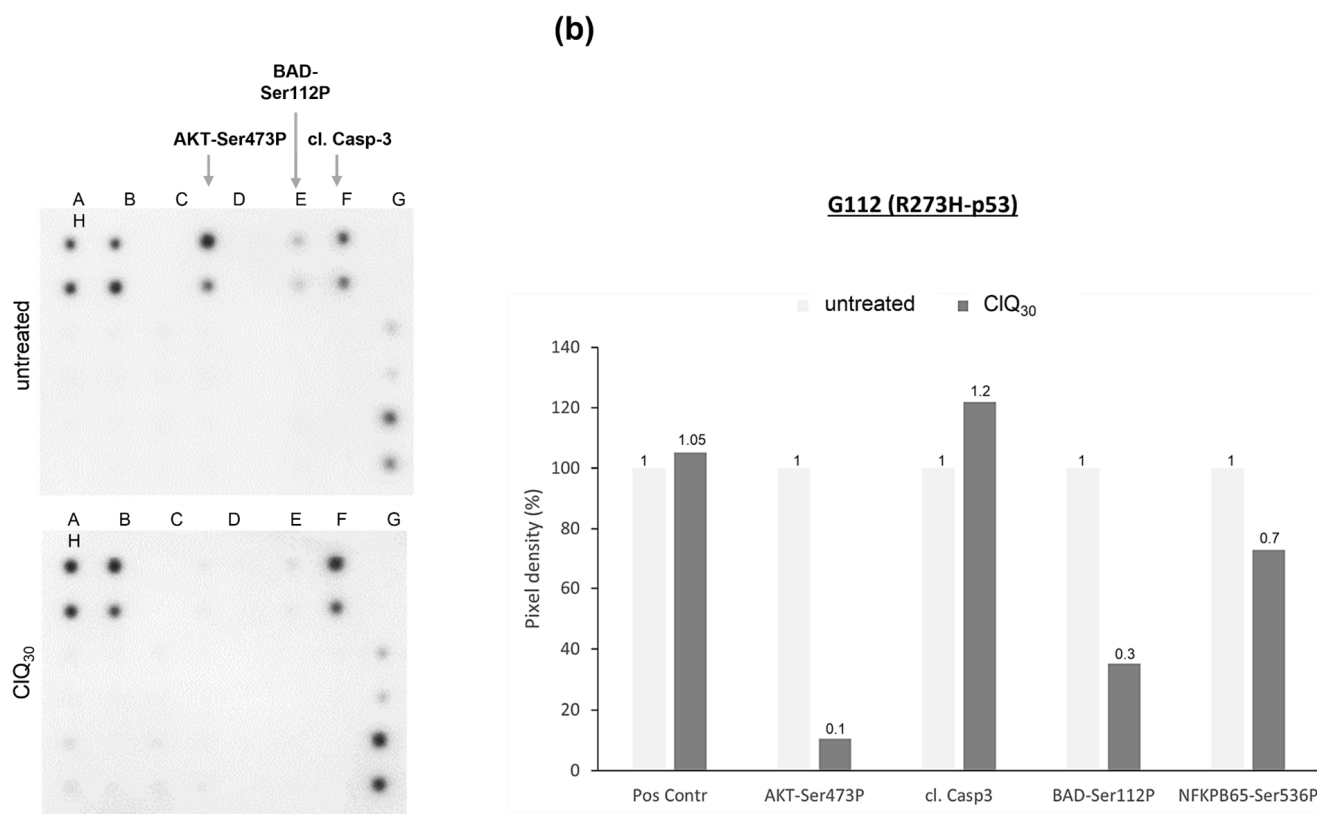


**Figure 9.** Effects of CIQ on apoptosis signaling pathways. Readouts from the APOSIG arrays incubated with cell lysates of (a) wtp53 or (b) R273H GSCs either untreated or treated with CIQ for 72 h and graphical presentation of the quantified readouts.

This effect was confirmed by western blot assessments showing that all tested GSCs, irrespective of their p53 status, undergo a drastic decline in the abundance of active AKT, AKT-Ser473P, upon the treatment with CIQ (Figure 10).

The reduction in AKT levels caused by CIQ occurred in all GSCs tested, indicating that this activity of CIQ is independent on the status of p53 and probably is conserved across different molecular subtypes of GSCs. Considering that AKT is the key factor promoting GB radioresistance, its reduction in CIQ-treated GSCs suggests that this mechanism might be involved in CIQ-mediated radiosensitization of glioma cells. This hypothesis is consistent with previous findings showing that AKT inhibition in conjunction with CIQ treatment sensitizes non-stem glioma cells to apoptosis [69], an effect that has been explained by autophagy-related impacts of CIQ known to impair the fusion between autophagosomes and lysosomes [69]. With this knowledge in mind, we sought to determine if CIQ-induced reduction in AKT levels occurs concurrently with the autophagic inhibition in GSCs. To that end, autophagy p62 and LC3BII were assessed in untreated and CIQ-treated GSCs. The results showed that CIQ treatment leads to a robust increase in both p62 and LC3BII in all GSCs tested (Figure 11).

These results indicate that CIQ-mediated blockage of autophagy and reduction in the abundance of active AKT occur concurrently in genetically distinct backgrounds and constitute conserved traits of CIQ actions in contrast to the variable effects of CIQ on transcription (Figure 8).

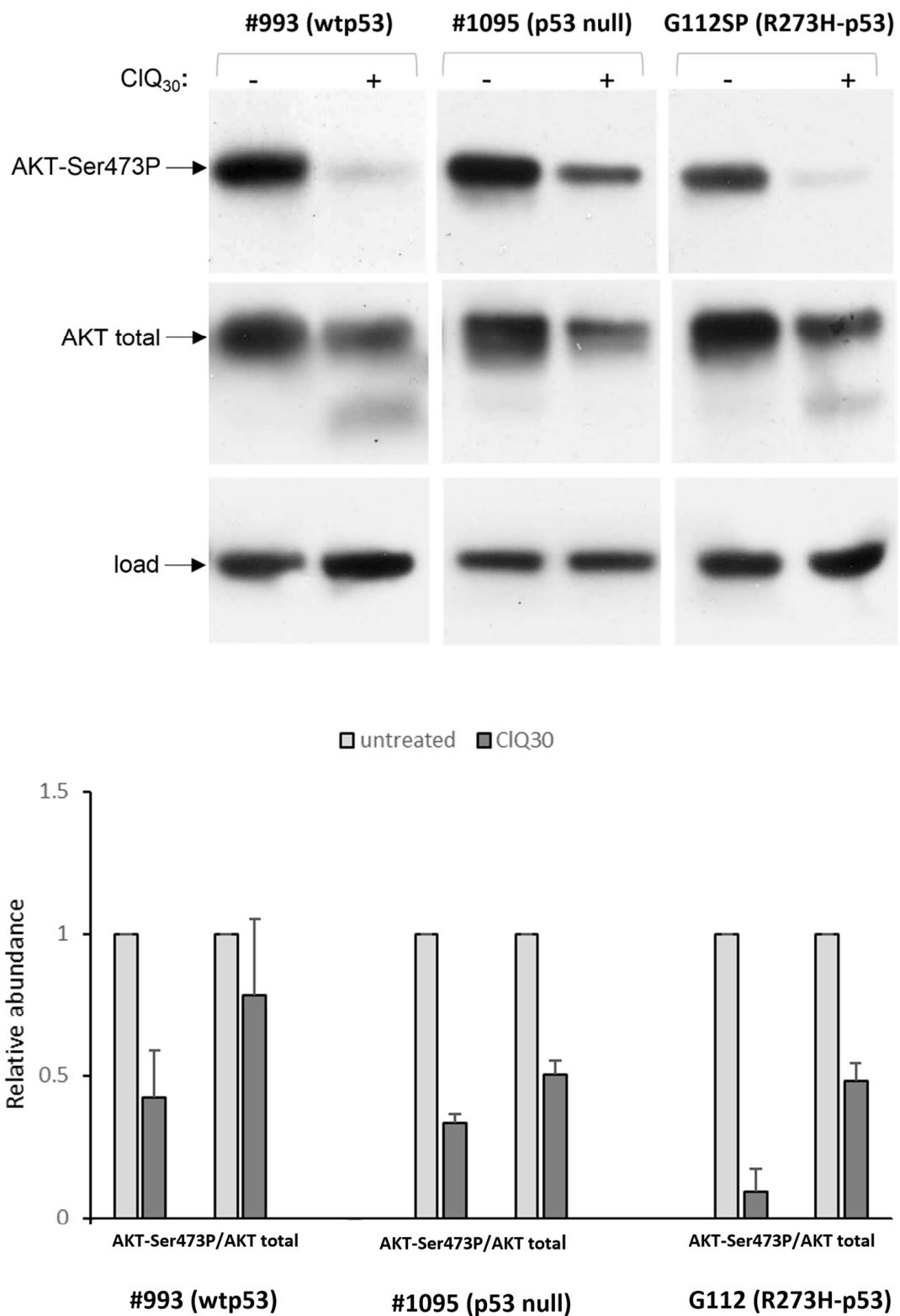


**Figure 10.** Effect of CIQ on the abundance of AKT kinase. Top panel shows representative blots for total HIPK2 and HIPK2-Tyr361P isoform in wtp53 (#993), R273H-p53 (G112) or p53-null GSCs after 72 h of treatment with CIQ. Graph shows the results of quantitative evaluations of datasets from independent experiments (n = 3 for each line) by densitometry. For total protein normalization, mitochondrial HSP70 or b-actin were used as internal loading controls.

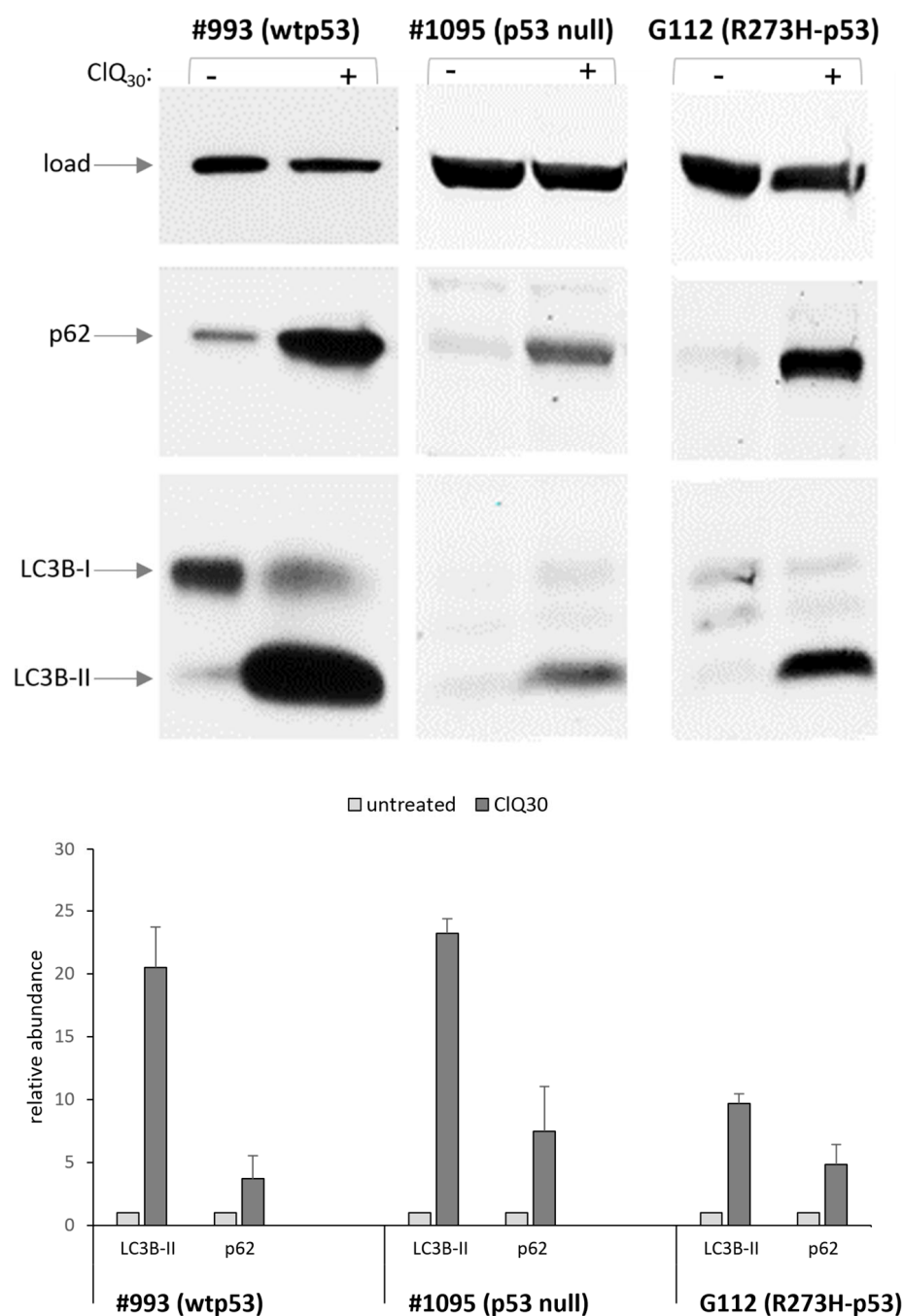


**Figure 11.** Effects of CIQ on the autophagic activity in GSCs differing for p53 status. Western blot assessments of late autophagy markers p63 and LC3B-II in untreated or CIQ-treated (72 h) GSCs. Protein loading was ascertained by probing for  $\beta$ -actin.

#### 4. Discussion

This study reports on molecular and cellular outcomes elicited by a putative radiosensitizer CIQ in human GSCs in vitro and in vivo. Our investigations reveal a high degree of functional and mechanistic versatility of CIQ in concurrent activation of pro-survival and pro-death signaling via transcriptional alterations and direct impacts on the abundance of proteins involved in cell fate determination. We provide evidence indicating that p53 status has a decisive impact on transcriptional changes induced by CIQ. In GSCs with wtp53, the transcriptional response induced by CIQ is primarily determined by p53-dependent transcriptional repression via the p53-p21-DREAM pathway [66,68] and p53-dependent transcriptional activation of glioma-promoting genes from the mevalonate pathway [70,71].

Our data reveal that CIQ-activated p53-dependent transcription differs in several aspects from the canonical mechanism of p53 activation by DNA damage. One is that p53 accumulation induced by CIQ does not involve post-translational modifications essential for p53 stabilization after DNA damage, such as phosphorylation of a p53-specific E3-ligase MDM2 on Ser395 [72,73]. Nor does it involve p53 phosphorylation on Ser46, a modification that promotes p53-dependent activation of apoptotic genes. We provide a mechanistic explanation for the lack of these regulatory modifications by uncovering a previously unknown impact of CIQ on the abundance of p53 regulatory kinases ATM and HIPK2, which are required for the execution of p53-dependent apoptosis [74–76]. The duality of CIQ manifests in its ability to induce p53 accumulation and to affect the abundance of ATM and HIPK2 at the same time. As these kinases are essential promoters of p53-dependent apoptosis, their decreased levels in CIQ-treated GSCs predict a selective weakening of pro-death but not pro-survival responses mediated by p53 via transcriptional regulation. Apart from its impacts on ATM and HIPK2, CIQ also affects the abundance of anti-apoptotic kinase AKT in company with inhibiting autophagy, a condition that induces death in non-stem glioma cells [69]. While our data support the hypothesis that concurrent inhibition of AKT and blockage of lysosomal degradation may promote glioma cells death [69], they also indicate that this mechanism is insufficient to suppress GSC-driven tumor growth in the absence of radiation. However, in the context of radiation treatment, the potential of CIQ to suppress tumor growth can become realized if its pro-survival activities mediated via wtp53 are “neutralized” by inactivating mutations in the TP53 gene. A similar conclusion has been reached in the study by Palanichamy et al., showing that GB radiosensitization via AKT silencing is only effective in the context of mutant p53 [77]. In the light of key AKT roles in GB radioresistance [77–82], our finding that CIQ affects the abundance of AKT supports the potential merit of CIQ as a radiosensitizing agent for GB. However, our data also indicate that CIQ-mediated radiosensitization is not a general phenomenon but a potential that can be realized depending on the p53 background, with mutated p53 emerging as a positive predictive factor for radiosensitization by CIQ. That the mere lack of p53 protein is insufficient to render GSC-driven tumors more susceptible to CIQ-mediated radiosensitization supports the view that specific activities of p53 mutant proteins should be taken into consideration when assessing the actionability of anti-cancer treatments [83]. From the mechanistic viewpoint, preferential sensitivity of GSC-driven tumors with mutated TP53 is consistent with the concept of synthetic lethality [84], whereby the combination of two inactivating events (p53 mutation and AKT inhibition, in the context of our study) is a prerequisite of effective outcome (CIQ-mediated tumor radiosensitization). The above interpretation relies on a premise that some common functions exerted by p53 and AKT should be impaired simultaneously to achieve the synthetic lethal effect. In this regard, DNA damage response (DDR) may be one of the intersecting points relevant for CIQ-mediated radiosensitization of GSC-driven tumors. Considering that DDR is the major mechanism by which both p53 and AKT protect cells from the killing effects of radiation [82,85–88], it is plausible to hypothesize that CIQ-mediated reduction in AKT in the background of DDR-impaired mutant p53 might create a condition for synthetic lethality from radiation and CIQ. As mutant p53 proteins are not simply inactive proteins but possess residual as well as diverse activities associated with “mutant p53 gain-of-function” [36–38], it will be important to clarify if a predisposition to CIQ-mediated radiosensitization is associated with all or only certain forms of mutant p53.

Basing on our findings, we propose a model in which the balance between inherently antagonistic impacts of CIQ on survival-promoting or death-inducing pathways is modulated by p53 (Figure 12).



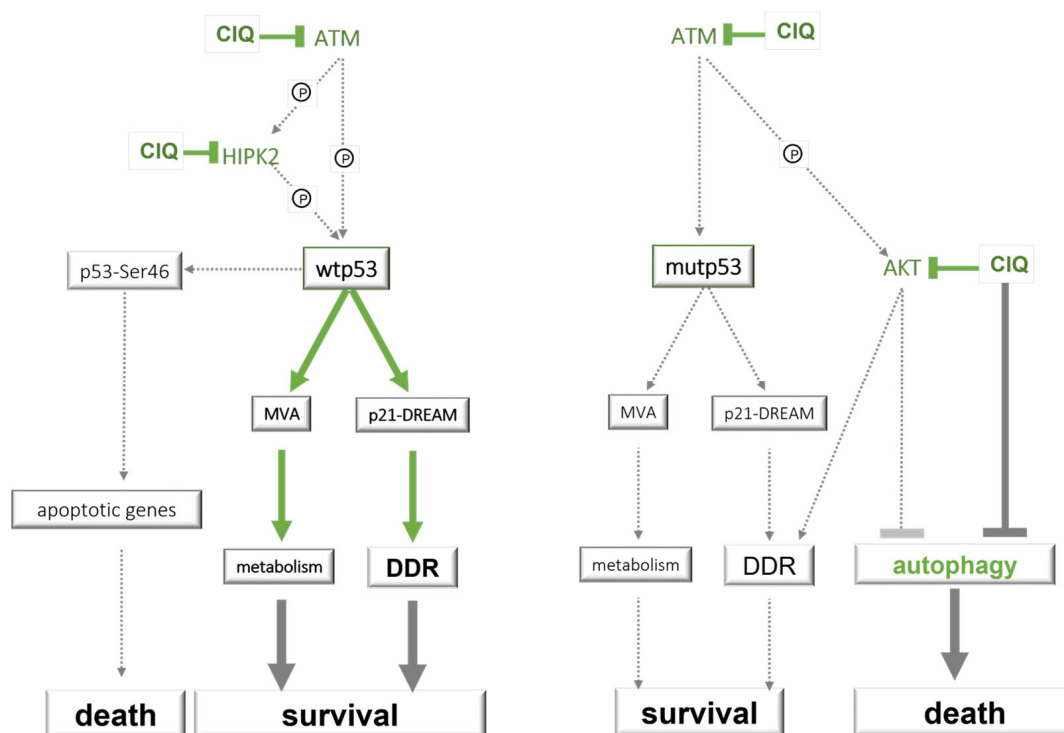


**Figure 12.** Schematic summary of main results integrated into the known networks of survival or death pathways. Green lines indicate molecular impacts of CIQ identified in this study. Solid and dashed indicate, respectively, sustained or diminished signaling in the context of wtp53 or transcriptionally impaired p53.

According to this model, functionality of transcriptional p53-p21-DREAM and p53-MVA axes has a decisive impact on the prevalence of pro-survival or pro-death outcomes that can be elicited by CIQ via p53-dependent and p53-independent mechanisms. In the wtp53 background, CIQ-mediated activation of survival-promoting pathways p21-DREAM and MVA serves as a counterbalance for pro-death signals elicited by CIQ via its p53-independent impacts on the abundance of cell fate regulators including ATM, AKT and HIPK2. In the background of mutant p53 with impaired potential to activate p21-DREAM and MVA pathways, pro-survival impacts of CIQ would prevail, a condition that gains special relevance in the context of radiation-induced DNA damage. As radiation itself is a potent activator of DDR, it could be envisaged that the combined action of CIQ and radiation treatment will augment the overall DDR capacity in the context of wtp53 but not in the context of transcriptionally impaired mutated p53. Indeed, transcriptomic changes induced by CIQ or radiation in wtp53 expressing GSCs show a striking overlap in differentially expressed genes, of which most are from the p21-DREAM pathway (Figure S11). The proposed model postulates that anti-tumor potential of CIQ has clinical relevance primarily in the context of radiation treatment and that impaired DDR is an important condition for CIQ-mediated tumor radiosensitization.

## 5. Conclusions

CIQ can activate both survival-promoting and survival-inhibiting responses in GSCs via transcription-dependent and transcription-independent mechanisms. Anti-tumor potential of CIQ has clinical relevance, primarily in the context of radiation. In the absence of radiation, the potential effectiveness of CIQ as monotherapy for GB is questionable or may even lead to unwanted outcomes. The ultimate outcome of CIQ impacts in radiated GSCs is determined by a balance between pro-death and pro-survival signals, elicited at the level of transcriptional control as well as via a direct impact on abundance of cell fate regulators including p53, HIPK2, AKT, and their common modulator ATM. Our data call for caution in

overinterpretation of in vitro effects of CIQ and emphasize the importance of in vivo testing with consideration of the impacts of the tumor microenvironment. Functionality of p53-p21-DREAM and p53-MVA axes has a decisive impact on the ultimate outcome exerted by CIQ with mutated p53 being a positive predictive factor CIQ-mediated radiosensitization.

**Supplementary Materials:** The following supporting information can be downloaded at: <https://www.mdpi.com/article/10.3390/cells12091290/s1>, Figure S1: GSC models used in the study. a, Nonsense mutation identified by genomic DNA sequencing in the TP53 exon 5 of GSC line #1095. wtp53 sequence from line #993 is shown as reference. b, Steady-state levels of the p53 protein determined by western blot using 20 and 30 µg total protein from each line. Consistent with an impaired turnover of mutant p53 proteins steady-state levels of p53-R273H are significantly higher compared to wtp53. c, Evaluations of self-renewal by determining the stem cell frequency (SCF) by ELDA. Graphical presentation of ELDA results and numerical estimates of SCF (red framed) with confidence intervals. d, Representative images of tumors arising from GSCs implanted into the brain of nude mice. Immunohistochemical staining for human nestin. Upper panel, whole brain images (magnification 1,6×). Bottom panel, enlarged images of brain-infiltrating tumor cells (magnification 20×). Figure S2: Schematic outline of in vivo experiments and experimental endpoints. a, Schematic presentation of the treatment protocol. “i.c. implantation”, intracranial implantation of GSCs. “frIR”, fractionated ionizing radiation. “CIQ”, chloroquine treatment via intraperitoneal route. “CIQ+frIR”, combined treatment with CIQ and frIR. “Sham”, control treatment using the same anesthesia protocol but no treatment with CIQ or frIR. b, Schematic presentation of brain-targeted irradiation using radiation-shielding lead plates. Figure S3: Assessments of proliferation in in vitro cultured GSCs. Representative images of untreated or CIQ-treated GSCs stained for proliferation marker Ki67 (red). Counterstaining by DAPI (blue). Magnification 20×. “Ab contr”, control staining with secondary antibodies only. Figure S4: Cell death assessments in in vitro cultured GSCs. Representative sub-G1 analyses of GSCs #993 (a), G112 (b) and #1095 (c) either untreated (“control”) or treated with CIQ, ionizing radiation (“IR”) or a combination of CIQ+IR for 72 h. Figure S5: Basal levels of ATM-Ser1981P in GSCs and non-stem glioma cells. Western blot for ATM-Ser1981P in untreated GSCs and non-stem glioma cells U87MG, either untreated or treated with ionizing radiation (7.5 Gy). 50 µg protein per lane. Protein loading ascertained by probing for β-actin. Figure S6: Differential effects of CIQ and radiation on ATM-Ser1981P in GSCs. a, western blot analysis of the full-length and truncated ATM proteins 24 or 48 hrs after CIQ treatment. b, time-course analysis of the full-length and truncated ATM proteins in wtp53 GSCs treated with increasing doses of radiation. Figures S7–S9: Processed data from comparative transcriptomic analyses of CIQ-treated vs. untreated GSCs. Differentially expressed genes identified in GSCs expressing wtp53 (S7), R273H-p53 (S8) or lacking p53 protein (S9). Figure S10: Schematic presentation of the APOSIG-Array. Antibodies specific for indicated proteins are spotted in duplicate. POS = Positive Control Spots, NEG = Negative Control Spots blot analysis. Figure S11: Cooperative activation of the p21-DREAM pathway in GSCs with wtp53 by CIQ and radiation. Venn diagrams of differentially expressed genes identified in wtp53 GSCs treated with CIQ (blue circles) or IR (red squares). Encircled is the number of common DEGs identified in both CIQ- and IR-GSCs. The majority of common DEGs belong to the p53-p21-DREAM pathway; Table S1: List of previously known glioblastoma-associated genes [89–104] identified as CIQ-DEGs in p53 null GSCs.

**Author Contributions:** Conceptualization, A.G., S.R.K., W.S.-S. and E.L.K.; formal analysis, E.L.K., G.S. and L.O.; investigation, A.M., N.B., F.J., B.L., B.S., G.S., L.O. and W.S.-S.; resources, A.G. and S.R.K.; data curation, G.S., L.O. and E.L.K.; writing—original draft preparation, E.L.K.; writing—review and editing, P.W., A.G. and W.S.-S.; supervision, E.L.K.; project administration, E.L.K. and A.G.; funding acquisition, E.L.K., P.W. and A.M. All authors have read and agreed to the published version of the manuscript.

**Funding:** This research was funded by the Monika-Kutzner Foundation (P.W., grant number 16082018) and FAZIT Foundation (A.M., grant number 09092021).

**Institutional Review Board Statement:** The animal study protocol was approved by the Ethics Committees of the University Medical Centre of Göttingen (permission #33.942502) and Translational Animal Research Center (TARC) of the Johannes Gutenberg University Medical Centre of Mainz (permission #23 177-07/G19-1-014).

**Informed Consent Statement:** Not applicable.

**Data Availability Statement:** Gene expression data and results of bioinformatic analyses are deposited in Gene Expression Omnibus database and can be found under the accession number GSE225191.

**Acknowledgments:** We thank Margret Rave-Fraenk, Christoph Schmitz-Salue and Mirjam Renovanz for the help with animal experiments.

**Conflicts of Interest:** The authors declare no conflict of interest.

## References

1. Wen, P.Y.; Weller, M.; Lee, E.Q.; Alexander, B.M.; Barnholtz-Sloan, J.S.; Barthel, F.P.; Batchelor, T.T.; Bindra, R.S.; Chang, S.M.; Chiocca, E.A.; et al. Glioblastoma in adults: A Society for Neuro-Oncology (SNO) and European Society of Neuro-Oncology (EANO) consensus review on current management and future directions. *Neuro-Oncol.* **2020**, *22*, 1073–1113. [[CrossRef](#)] [[PubMed](#)]
2. Weller, M.; van den Bent, M.; Preusser, M.; Le Rhun, E.; Tonn, J.C.; Minniti, G.; Bendszus, M.; Balana, C.; Chinot, O.; Dirven, L.; et al. EANO guidelines on the diagnosis and treatment of diffuse gliomas of adulthood. *Nat. Rev. Clin. Oncol.* **2021**, *18*, 170–186. [[CrossRef](#)] [[PubMed](#)]
3. Delgado-López, P.; Corrales-García, E. Survival in glioblastoma: A review on the impact of treatment modalities. *Clin. Transl. Oncol.* **2016**, *18*, 1062–1071. [[CrossRef](#)] [[PubMed](#)]
4. Oliver, L.; Lalier, L.; Salaud, C.; Heymann, D.; Cartron, P.F.; Vallette, F.M. Drug resistance in glioblastoma: Are persisters the key to therapy? *Cancer Drug Resist.* **2020**, *3*, 287. [[CrossRef](#)] [[PubMed](#)]
5. Stupp, R.; Hegi, M.E.; Mason, W.P.; van den Bent, M.J.; Taphoorn, M.J.B.; Janzer, R.C.; Ludwin, S.K.; Allgeier, A.; Fisher, B.; Belanger, K.; et al. Effects of radiotherapy with concomitant and adjuvant temozolomide versus radiotherapy alone on survival in glioblastoma in a randomised phase III study: 5-year analysis of the EORTC-NCIC trial. *Lancet Oncol.* **2009**, *10*, 459–466. [[CrossRef](#)]
6. Hegi, M.E.; Diserens, A.C.; Gorlia, T.; Hamou, M.F.; De Tribolet, N.; Weller, M.; Kros, J.M.; Hainfellner, J.A.; Mason, W.; Mariani, L.; et al. MGMT gene silencing and benefit from temozolomide in glioblastoma. *N. Engl. J. Med.* **2005**, *352*, 997–1003. [[CrossRef](#)]
7. Shergalis, A.; Bankhead, A., 3rd; Luesakul, U.; Muangsins, N.; Neamati, N. Current Challenges and Opportunities in Treating Glioblastoma. *Pharmacol. Rev.* **2018**, *70*, 412–445. [[CrossRef](#)]
8. Pearson, J.R.D.; Regad, T. Targeting cellular pathways in glioblastoma multiforme. *Signal Transduct. Target. Ther.* **2017**, *2*, 17040. [[CrossRef](#)]
9. Gimple, R.C.; Bhargava, S.; Dixit, D.; Rich, J.N. Glioblastoma stem cells: Lessons from the tumor hierarchy in a lethal cancer. *Genes Dev.* **2019**, *33*, 591–609. [[CrossRef](#)]
10. Bao, S.; Wu, Q.; McLendon, R.E.; Hao, Y.; Shi, Q.; Hjelmeland, A.B.; Dewhirst, M.W.; Bigner, D.D.; Rich, J.N. Glioma stem cells promote radioresistance by preferential activation of the DNA damage response. *Nature* **2006**, *444*, 756–760. [[CrossRef](#)]
11. Osuka, S.; Van Meir, E.G. Overcoming therapeutic resistance in glioblastoma: The way forward. *J. Clin. Investig.* **2017**, *127*, 415–426. [[CrossRef](#)] [[PubMed](#)]
12. Pascolo, S. Time to use a dose of Chloroquine as an adjuvant to anti-cancer chemotherapies. *Eur. J. Pharmacol.* **2016**, *771*, 139–144. [[CrossRef](#)] [[PubMed](#)]
13. Weyerhäuser, P.; Kantelhardt, S.R.; Kim, E.L. Re-purposing Chloroquine for Glioblastoma: Potential Merits and Confounding Variables. *Front. Oncol.* **2018**, *8*, 335. [[CrossRef](#)]
14. Bilger, A.; Bittner, M.I.; Grosu, A.L.; Wiedenmann, N.; Meyer, P.T.; Firat, E.; Milanovic, D. FET-PET-based reirradiation and chloroquine in patients with recurrent glioblastoma: First tolerability and feasibility results. *Strahlenther. Onkol.* **2014**, *190*, 957–961. [[CrossRef](#)] [[PubMed](#)]
15. Sotelo, J.; Briceño, E.; López-González, M.A. Adding chloroquine to conventional treatment for glioblastoma multiforme: A randomized, double-blind, placebo-controlled trial. *Ann. Intern. Med.* **2006**, *144*, 337–343. [[CrossRef](#)]
16. Briceño, E.; Reyes, S.; Sotelo, J. Therapy of glioblastoma multiforme improved by the antimutagenic chloroquine. *Neurosurg. Focus.* **2003**, *14*, 1–6. [[CrossRef](#)]
17. Compter, I.; Eekers, D.B.P.; Hoeben, A.; Rouschop, K.M.A.; Reymen, B.; Ackermans, L.; Beckervordersantforth, J.; Bauer, N.J.C.; Anten, M.M.; Wesseling, P.; et al. Chloroquine combined with concurrent radiotherapy and temozolomide for newly diagnosed glioblastoma: A phase IB trial. *Autophagy* **2021**, *17*, 2604–2612. [[CrossRef](#)]
18. Sotelo, J. *Chloroquine for Treatment of Glioblastoma Multiforme (NCT00224978)*; U.S. National Library of Medicine: Bethesda, MD, USA, 2009. Available online: <https://ClinicalTrials.gov/> (accessed on 1 March 2023).
19. DeNittis, A. *IDO2 Genetic Status Informs the Neoadjuvant Efficacy of Chloroquine (CQ) in Brain Metastasis Radiotherapy (NCT01727531)*; U.S. National Library of Medicine: Bethesda, MD, USA, 2015. Available online: <https://ClinicalTrials.gov/> (accessed on 1 March 2023).
20. Rodríguez, O.G.A. *Study of Whole-Brain Irradiation with Chloroquine for Brain Metastases (CLQ) (NCT01894633)*; U.S. National Library of Medicine: Bethesda, MD, USA, 2017. Available online: <https://ClinicalTrials.gov/> (accessed on 1 March 2023).

21. Wilmink, J.W. *Metformin and Chloroquine in IDH1/2-Mutated Solid Tumors (MACIST) (NCT02496741)*; U.S. National Library of Medicine: Bethesda, MD, USA, 2020. Available online: <https://ClinicalTrials.gov/> (accessed on 1 March 2023).
22. De Ruysscher, D. *The Addition of Chloroquine to Chemoradiation for Glioblastoma (CHLOROBRAIN) (NCT02378532)*; U.S. National Library of Medicine: Bethesda, MD, USA, 2020. Available online: <https://ClinicalTrials.gov/> (accessed on 1 March 2023).
23. Azab, M.A. *Chloroquine for Glioblastoma (NCT04772846)*; U.S. National Library of Medicine: Bethesda, MD, USA, 2021. Available online: <https://ClinicalTrials.gov/> (accessed on 1 March 2023).
24. Kramm, C. *International Cooperative Phase III Trial of the HIT-HGG Study Group (HIT-HGG-2013) (HIT-HGG-2013) (NCT03243461)*; U.S. National Library of Medicine: Bethesda, MD, USA, 2022. Available online: <https://ClinicalTrials.gov/> (accessed on 1 March 2023).
25. Lambin, P. *The Addition of Chloroquine to Chemoradiation for Glioblastoma (NCT02432417)*; U.S. National Library of Medicine: Bethesda, MD, USA, 2022. Available online: <https://ClinicalTrials.gov/> (accessed on 1 March 2023).
26. Dominello, M.; Partial Brain, R.T. *Temozolomide, Chloroquine, and TTF Therapy for the Treatment of Newly Diagnosed Glio-Blastoma (NCT04397679)*; U.S. National Library of Medicine: Bethesda, MD, USA, 2022. Available online: <https://ClinicalTrials.gov/> (accessed on 1 March 2023).
27. Maycotte, P.; Aryal, S.; Cummings, C.T.; Thorburn, J.; Morgan, M.J.; Thorburn, A. Chloroquine sensitizes breast cancer cells to chemotherapy independent of autophagy. *Autophagy* **2012**, *8*, 200–212. [[CrossRef](#)]
28. Eng, C.H.; Wang, Z.; Tkach, D.; Toral-Barza, L.; Ugwonali, S.; Liu, S.; Fitzgerald, S.L.; George, E.; Frias, E.; Cochran, N.; et al. Macroautophagy is dispensable for growth of KRAS mutant tumors and chloroquine efficacy. *Proc. Natl. Acad. Sci. USA* **2016**, *113*, 182–187. [[CrossRef](#)]
29. King, M.; Ganley, I.; Flemington, V. Inhibition of cholesterol metabolism underlies synergy between mTOR pathway inhibition and chloroquine in bladder cancer cells. *Oncogene* **2016**, *35*, 4518–4528. [[CrossRef](#)]
30. Kim, E.L.; Wüstenberg, R.; Rübsam, A.; Schmitz-Salue, C.; Warnecke, G.; Bücker, E.-M.; Pettkus, N.; Speidel, D.; Rohde, V.; Schulz-Schaeffer, W.; et al. Chloroquine activates the p53 pathway and induces apoptosis in human glioma cells. *Neuro-Oncology* **2010**, *12*, 389–400. [[CrossRef](#)] [[PubMed](#)]
31. Burikhanov, R.; Hebbar, N.; Noothi, S.K.; Shukla, N.; Sledziona, J.; Araujo, N.; Kudrimoti, M.; Wang, Q.J.; Watt, D.S.; Welch, D.R.; et al. Chloroquine-Inducible Par-4 Secretion Is Essential for Tumor Cell Apoptosis and Inhibition of Metastasis. *Cell Rep.* **2017**, *18*, 508–519. [[CrossRef](#)] [[PubMed](#)]
32. Park, E.J.; Min, K.-J.; Choi, K.S.; Kubatka, P.; Kruzliak, P.; Kim, D.E.; Kwon, T.K. Chloroquine enhances TRAIL-mediated apoptosis through up-regulation of DR5 by stabilization of mRNA and protein in cancer cells. *Sci. Rep.* **2016**, *6*, 22921. [[CrossRef](#)] [[PubMed](#)]
33. Hwang, J.R.; Kim, W.Y.; Cho, Y.J.; Ryu, J.Y.; Choi, J.J.; Jeong, S.Y.; Kim, M.S.; Kim, J.H.; Paik, E.S.; Lee, Y.Y.; et al. Chloroquine reverses chemoresistance via upregulation of p21WAF1/CIP1 and autophagy inhibition in ovarian cancer. *Cell Death Dis.* **2020**, *11*, 1034. [[CrossRef](#)] [[PubMed](#)]
34. Eloranta, K.; Cairo, S.; Liljeström, E.; Soini, T.; Kyrölähti, A.; Judde, J.-G.; Wilson, D.B.; Heikinheimo, M.; Pihlajoki, M. Chloroquine Triggers Cell Death and Inhibits PARPs in Cell Models of Aggressive Hepatoblastoma. *Front. Oncol.* **2020**, *10*, 1138. [[CrossRef](#)]
35. McLendon, R.; Friedman, A.; Bigneret, D.; Van Meir, E.G.; Brat, D.J.; Mastrogianakis, G.M.; Olson, J.J.; Mikkelsen, T.; Lehman, N.; Aldape, K.; et al. Comprehensive genomic characterization defines human glioblastoma genes and core pathways. *Nature* **2008**, *455*, 1061–1068.
36. Sabapathy, K.; Lane, D.P. Therapeutic targeting of p53: All mutants are equal, but some mutants are more equal than others. *Nat. Rev. Clin. Oncol.* **2018**, *15*, 13–30. [[CrossRef](#)]
37. Pfister, N.T.; Prives, C. Transcriptional Regulation by Wild-Type and Cancer-Related Mutant Forms of p53. *Cold Spring Harb. Perspect. Med.* **2017**, *7*, a026054. [[CrossRef](#)]
38. Mantovani, F.; Collavin, L.; Del Sal, G. Mutant p53 as a guardian of the cancer cell. *Cell Death Differ.* **2019**, *26*, 199–212. [[CrossRef](#)]
39. Hu, J.; Cao, J.; Topatana, W.; Juengpanich, S.; Li, S.; Bin Zhang, B.; Shen, J.; Cai, L.; Cai, X.; Chen, M. Targeting mutant p53 for cancer therapy: Direct and indirect strategies. *J. Hematol. Oncol.* **2021**, *14*, 157. [[CrossRef](#)]
40. Stupp, R.; Mason, W.P.; van den Bent, M.J.; Weller, M.; Fisher, B.; Taphoorn, M.J.B.; Belanger, K.; Brandes, A.A.; Marosi, C.; Bogdahn, U.; et al. Radiotherapy plus Concomitant and Adjuvant Temozolomide for Glioblastoma. *N. Engl. J. Med.* **2005**, *352*, 987–996. [[CrossRef](#)] [[PubMed](#)]
41. Barrantes-Freer, A.; Kim, E.; Bielanska, J.; Giese, A.; Mortensen, L.S.; Schulz-Schaeffer, W.J.; Stadelmann, C.; Brück, W.; Pardo, L.A. Human Glioma-Initiating Cells Show a Distinct Immature Phenotype Resembling but Not Identical to NG2 Glia. *J. Neuropathol. Exp. Neurol.* **2013**, *72*, 307–324. [[CrossRef](#)] [[PubMed](#)]
42. Barrantes-Freer, A.; Renovanz, M.; Eich, M.; Braukmann, A.; Sprang, B.; Spirin, P.; Pardo, L.A.; Giese, A.; Kim, E.L. CD133 Expression Is Not Synonymous to Immunoreactivity for AC133 and Fluctuates throughout the Cell Cycle in Glioma Stem-like Cells. *PLoS ONE* **2015**, *10*, e0130519. [[CrossRef](#)]
43. Kalasauskas, D.; Sorokin, M.; Sprang, B.; Elmasri, A.; Viehweg, S.; Salinas, G.; Opitz, L.; Rave-Fraenk, M.; Schulz-Schaeffer, W.; Kantelhardt, S.R.; et al. Diversity of Clinically Relevant Outcomes Resulting from Hypofractionated Radiation in Human Glioma Stem Cells Mirrors Distinct Patterns of Transcriptomic Changes. *Cancers* **2020**, *12*, 570. [[CrossRef](#)] [[PubMed](#)]
44. Fauß, J.; Sprang, B.; Leukel, P.; Sommer, C.; Nikolova, T.; Ringel, F.; Kim, E.L. ALDH1A3 Segregated Expression and Nucleus-Associated Proteasomal Degradation Are Common Traits of Glioblastoma Stem Cells. *Biomedicines* **2021**, *10*, 7. [[CrossRef](#)]



45. Hanisch, D.; Krumm, A.; Diehl, T.; Stork, C.M.; Dejung, M.; Butter, F.; Kim, E.; Brenner, W.; Fritz, G.; Hofmann, T.G.; et al. Class I HDAC overexpression promotes temozolomide resistance in glioma cells by regulating RAD18 ex-pression. *Cell Death Dis.* **2022**, *13*, 293. [[CrossRef](#)] [[PubMed](#)]
46. Kim, E.L.; Yoshizato, K.; Kluwe, L.; Meissner, H.; Warnecke, G.; Zapf, S.; Westphal, M.; Deppert, W.; Giese, A. Comparative assessment of the functional p53 status in glioma cells. *Anticancer Res.* **2005**, *25*, 213–224.
47. Hu, Y.; Smyth, G.K. ELDA: Extreme limiting dilution analysis for comparing depleted and enriched populations in stem cell and other assays. *J. Immunol. Methods* **2009**, *347*, 70–78. [[CrossRef](#)]
48. Kim, E.L.; Sorokin, M.; Kantelhardt, S.R.; Kalasauskas, D.; Sprang, B.; Fauss, J.; Ringel, F.; Garazha, A.; Albert, E.; Gaifullin, N.; et al. Intratumoral Heterogeneity and Longitudinal Changes in Gene Expression Predict Differential Drug Sensitivity in Newly Diagnosed and Recurrent Glioblastoma. *Cancers* **2020**, *12*, 520. [[CrossRef](#)]
49. Gautier, L.; Cope, L.; Bolstad, B.M.; Irizarry, R.A. Affy—Analysis of Affymetrix GeneChip data at the probe level. *Bioinformatics* **2004**, *20*, 307–315. [[CrossRef](#)]
50. Wettenhall, J.M.; Smyth, G.K. limmaGUI: A graphical user interface for linear modeling of microarray data. *Bioinformatics* **2004**, *20*, 3705–3706. [[CrossRef](#)] [[PubMed](#)]
51. Gentleman, R.C.; Carey, V.J.; Bates, D.M.; Bolstad, B.; Dettling, M.; Dudoit, S.; Ellis, B.; Gautier, L.; Ge, Y.; Gentry, J.; et al. Bioconductor: Open software development for computational biology and bioinformatics. *Genome Biol.* **2004**, *5*, R80. [[CrossRef](#)] [[PubMed](#)]
52. Smyth, G.K. Linear Models and Empirical Bayes Methods for Assessing Differential Expression in Microarray Experiments. *Stat. Appl. Genet. Mol. Biol.* **2004**, *3*, 3. [[CrossRef](#)] [[PubMed](#)]
53. Benjamini, Y.; Hochberg, Y. Controlling the False Discovery Rate: A Practical and Powerful Approach to Multiple Testing. *J. R. Stat. Soc. Ser. B* **1995**, *57*, 289–300. [[CrossRef](#)]
54. Golden, E.B.; Cho, H.-Y.; Jahanian, A.; Hofman, F.M.; Louie, S.G.; Schönthal, A.H.; Chen, T.C. Chloroquine enhances temozolomide cytotoxicity in malignant gliomas by blocking autophagy. *Neurosurg. Focus.* **2014**, *37*, E12. [[CrossRef](#)]
55. Ye, H.; Chen, M.; Cao, F.; Huang, H.; Zhan, R.; Zheng, X. Chloroquine, an autophagy inhibitor, potentiates the radiosensitivity of glioma initiating cells by inhibiting autophagy and activating apoptosis. *BMC Neurol.* **2016**, *16*, 178. [[CrossRef](#)]
56. Vessoni, A.T.; Quinet, A.; de Andrade-Lima, L.C.; Martins, D.J.; Garcia, C.C.M.; Rocha, C.R.R.; Vieira, D.B.; Menck, C.F.M. Chloroquine-induced glioma cells death is associated with mitochondrial membrane potential loss, but not oxidative stress. *Free. Radic. Biol. Med.* **2016**, *90*, 91–100. [[CrossRef](#)]
57. Geng, Y.; Kohli, L.; Klocke, B.J.; Roth, K.A. Chloroquine-induced autophagic vacuole accumulation and cell death in glioma cells is p53 independent. *Neuro-Oncology* **2010**, *12*, 473–481. [[CrossRef](#)]
58. Chen, P.; Luo, X.; Nie, P.; Wu, B.; Xu, W.; Shi, X.; Chang, H.; Li, B.; Yu, X.; Zou, Z. CQ synergistically sensitizes human colorectal cancer cells to SN-38/CPT-11 through lysosomal and mitochondrial apoptotic pathway via p53-ROS cross-talk. *Free. Radic. Biol. Med.* **2017**, *104*, 280–297. [[CrossRef](#)]
59. Lee, S.W.; Kim, H.-K.; Lee, N.-H.; Yi, H.-Y.; Kim, H.-S.; Hong, S.H.; Hong, Y.-K.; Joe, Y.A. The synergistic effect of combination temozolomide and chloroquine treatment is dependent on autophagy formation and p53 status in glioma cells. *Cancer Lett.* **2015**, *360*, 195–204. [[CrossRef](#)]
60. Bakkenist, C.J.; Kastan, M.B. DNA damage activates ATM through intermolecular autophosphorylation and dimer dissociation. *Nature* **2003**, *421*, 499–506. [[CrossRef](#)] [[PubMed](#)]
61. Shiloh, Y.; Ziv, Y. The ATM protein kinase: Regulating the cellular response to genotoxic stress, and more. *Nat. Rev. Mol. Cell Biol.* **2013**, *14*, 197–210. [[CrossRef](#)] [[PubMed](#)]
62. Maya, R.; Balass, M.; Kim, S.-T.; Shkedy, D.; Leal, J.-F.M.; Shifman, O.; Moas, M.; Buschmann, T.; Ronai, Z.; Shiloh, Y.; et al. ATM-dependent phosphorylation of Mdm2 on serine 395: Role in p53 activation by DNA damage. *Genes Dev.* **2001**, *15*, 1067–1077. [[CrossRef](#)] [[PubMed](#)]
63. Cheng, Q.; Chen, L.; Li, Z.; Lane, W.S.; Chen, J. ATM activates p53 by regulating MDM2 oligomerization and E3 processivity. *EMBO J.* **2009**, *28*, 3857–3867. [[CrossRef](#)]
64. Wang, J.; Pabla, N.; Wang, C.-Y.; Wang, W.; Schoenlein, P.V.; Dong, Z. Caspase-mediated cleavage of ATM during cisplatin-induced tubular cell apoptosis: Inactivation of its kinase activity toward p53. *Am. J. Physiol.-Ren. Physiol.* **2006**, *291*, F1300–F1307. [[CrossRef](#)] [[PubMed](#)]
65. Liebl, M.C.; Hofmann, T.G. Cell Fate Regulation upon DNA Damage: p53 Serine 46 Kinases Pave the Cell Death Road. *BioEssays* **2019**, *41*, e1900127. [[CrossRef](#)]
66. Engeland, K. Cell cycle arrest through indirect transcriptional repression by p53: I have a DREAM. *Cell Death Differ.* **2018**, *25*, 114–132. [[CrossRef](#)]
67. Engeland, K. Cell cycle regulation: p53-p21-RB signaling. *Cell Death Differ.* **2022**, *29*, 946–960. [[CrossRef](#)]
68. Fischer, M.; Grossmann, P.; Padi, M.; DeCaprio, J.A. Integration of TP53, DREAM, MMB-FOXM1 and RB-E2F target gene analyses identifies cell cycle gene regulatory networks. *Nucleic Acids Res.* **2016**, *44*, 6070–6086. [[CrossRef](#)]
69. Degtyarev, M.; De Mazière, A.; Orr, C.; Lin, J.; Lee, B.B.; Tien, J.Y.; Prior, W.W.; van Dijk, S.; Wu, H.; Gray, D.C.; et al. Akt inhibition promotes autophagy and sensitizes PTEN-null tumors to lysosomotropic agents. *J. Cell Biol.* **2008**, *183*, 101–116. [[CrossRef](#)]
70. Mullen, P.J.; Yu, R.; Longo, J.; Archer, M.C.; Penn, L.Z. The interplay between cell signalling and the mevalonate pathway in cancer. *Nat. Rev. Cancer* **2016**, *16*, 718–731. [[CrossRef](#)] [[PubMed](#)]



71. Laka, K.; Makgoo, L.; Mbita, Z. Cholesterol-Lowering Phytochemicals: Targeting the Mevalonate Pathway for Anticancer Interventions. *Front. Genet.* **2022**, *13*, 841639. [[CrossRef](#)] [[PubMed](#)]
72. Sparks, A.; Dayal, S.; Das, J.; Robertson, P.; Menendez, S.; Saville, M.K. The degradation of p53 and its major E3 ligase Mdm2 is differentially dependent on the proteasomal ubiquitin receptor S5a. *Oncogene* **2014**, *33*, 4685–4696. [[CrossRef](#)] [[PubMed](#)]
73. Carr, M.I.; Roderick, J.E.; Gannon, H.S.; Kelliher, M.A.; Jones, S.N. Mdm2 Phosphorylation Regulates Its Stability and Has Contrasting Effects on Oncogene and Radiation-Induced Tumorigenesis. *Cell Rep.* **2016**, *16*, 2618–2629. [[CrossRef](#)]
74. Hofmann, T.G.; Möller, A.; Sirma, H.; Zentgraf, H.; Taya, Y.; Dröge, W.; Will, H.; Schmitz, M.L. Regulation of p53 activity by its interaction with homeodomain-interacting protein kinase-2. *Nature* **2002**, *4*, 1–10. [[CrossRef](#)] [[PubMed](#)]
75. Hofmann, T.G.; Glas, C.; Bitomsky, N. HIPK2: A tumour suppressor that controls DNA damage-induced cell fate and cytokinesis. *BioEssays* **2013**, *35*, 55–64. [[CrossRef](#)] [[PubMed](#)]
76. Conrad, E.; Polonio-Vallon, T.; Meister, M.; Matt, S.; Bitomsky, N.; Herbel, C.; Liebl, M.; Greiner, V.; Kriznik, B.; Schumacher, S.; et al. HIPK2 restricts SIRT1 activity upon severe DNA damage by a phosphorylation-controlled mechanism. *Cell Death Differ.* **2016**, *23*, 110–122. [[CrossRef](#)] [[PubMed](#)]
77. Palanichamy, K.; Patel, D.; Jacob, J.R.; Litzenberg, K.T.; Gordon, N.; Acus, K.; Noda, S.-E.; Chakravarti, A. Lack of Constitutively Active DNA Repair Sensitizes Glioblastomas to Akt Inhibition and Induces Synthetic Lethality with Radiation Treatment in a p53-Dependent Manner. *Mol. Cancer Ther.* **2018**, *17*, 336–346. [[CrossRef](#)]
78. Liu, Q.; Turner, K.M.; Yung, W.K.A.; Chen, K.; Zhang, W. Role of AKT signaling in DNA repair and clinical response to cancer therapy. *Neuro-Oncology* **2014**, *16*, 1313–1323. [[CrossRef](#)]
79. Alemi, F.; Sadigh, A.R.; Malakoti, F.; Elhaei, Y.; Ghaffari, S.H.; Maleki, M.; Asemi, Z.; Yousefi, B.; Targhazeh, N.; Majidinia, M. Molecular mechanisms involved in DNA repair in human cancers: An overview of PI3k/Akt signaling and PIKKs crosstalk. *J. Cell. Physiol.* **2022**, *237*, 313–328. [[CrossRef](#)]
80. Han, X.; Xue, X.; Zhou, H.; Zhang, G. A molecular view of the radioresistance of gliomas. *Oncotarget* **2017**, *8*, 100931–100941. [[CrossRef](#)] [[PubMed](#)]
81. Ali, M.Y.; Oliva, C.R.; Noman, A.S.M.; Allen, B.G.; Goswami, P.C.; Zakharia, Y.; Monga, V.; Spitz, D.R.; Buatti, J.M.; Griguer, C.E. Radioresistance in Glioblastoma and the Development of Radiosensitizers. *Cancers* **2020**, *12*, 2511. [[CrossRef](#)] [[PubMed](#)]
82. Turner, K.M.; Sun, Y.; Ji, P.; Granberg, K.J.; Bernard, B.; Hu, L.; Cogdell, D.E.; Zhou, X.; Yli-Harja, O.; Nykter, M.; et al. Genomically amplified Akt3 activates DNA repair pathway and promotes glioma progression. *Proc. Natl. Acad. Sci. USA* **2015**, *112*, 3421–3426. [[CrossRef](#)]
83. Hassin, O.; Nataraj, N.B.; Shreberk-Shaked, M.; Aylon, Y.; Yaeger, R.; Fontemaggi, G.; Mukherjee, S.; Maddalena, M.; Avioz, A.; Iancu, O.; et al. Different hotspot p53 mutants exert distinct phenotypes and predict outcome of colorectal cancer patients. *Nat. Commun.* **2022**, *13*, 2800. [[CrossRef](#)] [[PubMed](#)]
84. Huang, A.; Garraway, L.A.; Ashworth, A.; Weber, B. Synthetic lethality as an engine for cancer drug target discovery. *Nat. Rev. Drug Discov.* **2020**, *19*, 23–38. [[CrossRef](#)] [[PubMed](#)]
85. Kruiswijk, F.; Labuschagne, C.F.; Vousden, K.H. p53 in survival, death and metabolic health: A lifeguard with a licence to kill. *Nat. Rev. Mol. Cell Biol.* **2015**, *16*, 393–405. [[CrossRef](#)]
86. Lukin, D.J.; Carvajal, L.A.; Liu, W.-J.; Resnick-Silverman, L.; Manfredi, J.J. p53 Promotes Cell Survival due to the Reversibility of Its Cell-Cycle Checkpoints. *Mol. Cancer Res.* **2015**, *13*, 16–28. [[CrossRef](#)]
87. Kao, G.D.; Jiang, Z.; Fernandes, A.M.; Gupta, A.K.; Maity, A. Inhibition of Phosphatidylinositol-3-OH Kinase/Akt Signaling Impairs DNA Repair in Glioblastoma Cells following Ionizing Radiation. *J. Biol. Chem.* **2007**, *282*, 21206–21212. [[CrossRef](#)]
88. Golding, S.E.; Morgan, R.N.; Adams, B.R.; Hawkins, A.J.; Povirk, L.F.; Valerie, K. Pro-survival AKT and ERK signaling from EGFR and mutant EGFRvIII enhances DNA double-strand break repair in human glioma cells. *Cancer Biol. Ther.* **2009**, *8*, 730–738. [[CrossRef](#)]
89. Zhuo, S.; Chen, Z.; Yang, Y.; Zhang, J.; Tang, J.; Yang, K. Clinical and Biological Significances of a Ferroptosis-Related Gene Signature in Glioma. *Front. Oncol.* **2020**, *10*, 590861. [[CrossRef](#)]
90. Goplen, D.; Bougnaud, S.; Rajcevic, U.; Bøe, S.O.; Skaftnesmo, K.O.; Voges, J.; Enger, P.; Wang, J.; Tysnes, B.B.; Laerum, O.D.; et al.  $\alpha$ B-crystallin is elevated in highly infiltrative apoptosis-resistant glioblastoma cells. *Am. J. Pathol.* **2010**, *177*, 1618–1628. [[CrossRef](#)] [[PubMed](#)]
91. Foltyn, M.; Luger, A.-L.; Lorenz, N.I.; Sauer, B.; Mittelbronn, M.; Harter, P.N.; Steinbach, J.P.; Ronellenfitsch, M.W. The physiological mTOR complex 1 inhibitor DDIT4 mediates therapy resistance in glioblastoma. *Br. J. Cancer* **2019**, *120*, 481–487. [[CrossRef](#)] [[PubMed](#)]
92. Lewis, C.A.; Brault, C.; Peck, B.; Bensaad, K.; Griffiths, B.; Mitter, R.; Chakravarty, P.; East, P.; Dankworth, B.; Alibhai, D.; et al. SREBP maintains lipid biosynthesis and viability of cancer cells under lipid- and oxygen-deprived conditions and defines a gene signature associated with poor survival in glioblastoma multiforme. *Oncogene* **2015**, *34*, 5128–5140. [[CrossRef](#)] [[PubMed](#)]
93. Guo, L.; Chen, Y.; Hu, S.; Gao, L.; Tang, N.; Liu, R.; Qin, Y.; Ren, C.; Du, S. GDF15 expression in glioma is associated with malignant progression, immune microenvironment, and serves as a prognostic factor. *CNS Neurosci. Ther.* **2022**, *28*, 158–171. [[CrossRef](#)]
94. Feng, X.; Zhang, L.; Ke, S.; Liu, T.; Hao, L.; Zhao, P.; Tu, W.; Cang, S. High expression of GPNMB indicates an unfavorable prognosis in glioma: Combination of data from the GEO and CGGA databases and validation in tissue microarray. *Oncol. Lett.* **2020**, *20*, 2356–2368. [[CrossRef](#)]

95. Akçay, S.; Güven, E.; Afzal, M.; Kazmi, I. Non-negative matrix factorization and differential expression analyses identify hub genes linked to progression and prognosis of glioblastoma multiforme. *Gene* **2022**, *824*, 146395. [[CrossRef](#)]
96. Delic, S.; Lottmann, N.; Jetschke, K.; Reifenberger, G.; Riemenschneider, M.J. Identification and functional validation of CDH11, PCSK6 and SH3GL3 as novel glioma invasion-associated candidate genes. *Neuropathol. Appl. Neurobiol.* **2012**, *38*, 201–212. [[CrossRef](#)]
97. He, Z.; You, C.; Zhao, D. Long non-coding RNA UCA1/miR-182/PFKFB2 axis modulates glioblastoma-associated stromal cells-mediated glycolysis and invasion of glioma cells. *Biochem. Biophys. Res. Commun.* **2018**, *500*, 569–576. [[CrossRef](#)]
98. Putthisen, S.; Silsirivanit, A.; Panawan, O.; Niibori-Nambu, A.; Nishiyama-Ikeda, Y.; Ma-In, P.; Luang, S.; Ohta, K.; Muisuk, K.; Wongkham, S.; et al. Targeting alpha2,3-sialylated glycan in glioma stem-like cells by Maackia amurensis lectin-II: A promising strategy for glioma treatment. *Exp. Cell Res.* **2022**, *410*, 112949. [[CrossRef](#)]
99. Mariani, L.; Beaudry, C.; McDonough, W.S.; Hoelzinger, D.B.; Demuth, T.; Ross, K.R.; Berens, T.; Coons, S.W.; Watts, G.; Trent, J.M.; et al. Glioma Cell Motility is Associated with Reduced Transcription of Proapoptotic and Proliferation Genes: A cDNA Microarray Analysis. *J. Neurooncol.* **2001**, *53*, 161–176. [[CrossRef](#)]
100. Sachdeva, R.; Wu, M.; Smiljanic, S.; Kaskun, O.; Ghannad-Zadeh, K.; Celebre, A.; Isaev, K.; Morrissy, A.S.; Guan, J.; Tong, J.; et al. ID1 Is Critical for Tumorigenesis and Regulates Chemoresistance in Glioblastoma. *Cancer Res.* **2019**, *79*, 4057–4071. [[CrossRef](#)] [[PubMed](#)]
101. Nair, R.; Teo, W.S.; Mittal, V.; Swarbrick, A. ID proteins regulate diverse aspects of cancer progression and provide novel therapeutic opportunities. *Mol. Ther.* **2014**, *22*, 1407–1415. [[CrossRef](#)] [[PubMed](#)]
102. Dong, C.; Zhang, J.; Fang, S.; Liu, F. IGFBP5 increases cell invasion and inhibits cell proliferation by EMT and Akt signaling pathway in Glioblastoma multiforme cells. *Cell Div.* **2020**, *15*, 4. [[CrossRef](#)] [[PubMed](#)]
103. Serafim, R.B.; da Silva, P.; Cardoso, C.; Di Cristofaro, L.F.M.; Netto, R.P.; de Almeida, R.; Navegante, G.; Storti, C.B.; de Sousa, J.F.; de Souza, F.C.; et al. Expression Profiling of Glioblastoma Cell Lines Reveals Novel Extracellular Matrix-Receptor Genes Correlated With the Responsiveness of Glioma Patients to Ionizing Radiation. *Front. Oncol.* **2021**, *11*, 668090. [[CrossRef](#)] [[PubMed](#)]
104. Hjelmeland, A.B.; Wu, Q.; Wickman, S.; Eyster, C.; Heddleston, J.; Shi, Q.; Lathia, J.D.; Macsworlds, J.; Lee, J.; McLendon, R.E.; et al. Targeting A20 decreases glioma stem cell survival and tumor growth. *PLoS Biol.* **2010**, *8*, e1000319. [[CrossRef](#)]

**Disclaimer/Publisher's Note:** The statements, opinions and data contained in all publications are solely those of the individual author(s) and contributor(s) and not of MDPI and/or the editor(s). MDPI and/or the editor(s) disclaim responsibility for any injury to people or property resulting from any ideas, methods, instructions or products referred to in the content.